

Westinghouse Nuclear Energy Systems



WCAP-9520

WESTINGHOUSE CLASS 3
CUSTOMER DESIGNATED DISTRIBUTION

ANALYSIS OF CAPSULE F FROM THE SOUTHERN
CALIFORNIA EDISON COMPANY

SAN ONOFRE REACTOR VESSEL
RADIATION SURVEILLANCE PROGRAM

S. E. Yanichko
S. L. Anderson
W. T. Kaiser

May 1979

APPROVED:


J. N. Chirigos, Manager
Structural Materials Engineering

Prepared by Westinghouse for the
Southern California Edison Company

Work Performed Under EZGP 200

Although the information contained in this report is nonproprietary,
no distribution shall be made outside Westinghouse or its Licensees
without the customer's approval.

WESTINGHOUSE ELECTRIC CORPORATION
Nuclear Energy Systems
P. O. Box 355
Pittsburgh, Pennsylvania 15230

8004240397

LIST OF ILLUSTRATIONS

Figure	Title	Page
4-1	Arrangement of Surveillance Capsules in the San Onofre Reactor Vessel	4-2
4-2	Arrangement of Specimens, Thermal Monitors, and Dosimeters in Capsule F	4-5
5-1	Charpy V-Notch Impact Data for San Onofre Pressure Vessel Shell Plate W7601-8	5-3
5-2	Charpy V-Notch Impact Data for San Onofre Pressure Vessel Weld Metal	5-4
5-3	Charpy V-Notch Impact Data for San Onofre Pressure Vessel Weld Heat-Affected-Zone Metal	5-5
5-4	Charpy V-Notch Impact Data for A302 Grade B ASTM Correlation Monitor Material	5-6
5-5	Charpy Impact Specimen Fracture Surfaces for San Onofre Pressure Vessel Shell Plate W7601-8	5-10
5-6	Charpy Impact Specimen Fracture Surfaces for San Onofre Weld Metal	5-11
5-7	Charpy Impact Specimen Fracture Surfaces for San Onofre Weld Heat-Affected-Zone Metal	5-12
5-8	Charpy Impact Specimen Fracture Surfaces for A302 Grade B ASTM Correlation Monitor Material	5-13
5-9	Tensile Properties for San Onofre Pressure Vessel Shell Plate W7601-8	5-17
5-10	Tensile Properties for San Onofre Weld Metal	5-18
5-11	Fractured Tensile Specimens From San Onofre Shell Plate W7601-8	5-20
5-12	Fractured Tensile Specimens From San Onofre Weld Metal	5-21
5-13	Typical Stress-Strain Curve for Tension Specimens (Tension Specimen No. YB-6)	5-22

TABLE OF CONTENTS

Section	Title	Page
1	SUMMARY	1-1
2	INTRODUCTION	2-1
3	BACKGROUND	3-1
4	DESCRIPTION OF PROGRAM	4-1
5	TESTING OF SPECIMENS FROM CAPSULE F	5-1
	5-1. Test Procedure	5-1
	5-2. Charpy V-Notch Impact Test Results	5-2
	5-3. Tensile Test Results	5-15
	5-4. Wedge Opening Loading Tests	5-15
6	NEUTRON DOSIMETRY ANALYSIS	6-1
	6-1. Description of Neutron Flux Monitors	6-1
	6-2. Analytical Procedures	6-3
	6-3. Results of Analysis	6-6
Appendix A	HEATUP AND COOLDOWN LIMIT CURVES FOR NORMAL OPERATION	A-1
	A-1. Introduction	A-1
	A-2. Fracture Toughness Properties	A-1
	A-3. Criteria for Allowable Pressure-Temperature Relationships	A-6
	A-4. Heatup and Cooldown Limit Curves	A-8

LIST OF ILLUSTRATIONS (cont)

Figure	Title	Page
6-1	Calculated Azimuthal Distribution on Neutron Flux ($E > 1$ Mev) at the Core Midplane of the San Onofre Reactor Vessel	6-14
6-2	Relative Axial Variation of Fast Neutron Flux ($E > 1.0$ Mev) Incident on the San Onofre Reactor Vessel	6-15
6-3	Calculated Maximum End-of-Life Fast Neutron Fluence ($E > 1$ Mev) as a Function of Radius Within the San Onofre Reactor Vessel	6-16
A-1	Effect of Fluence and Copper Content on ΔRT_{NDT} for Reactor Vessel Steels Exposed to Irradiation at $550^{\circ}F$	A-2
A-2	Fast Neutron Fluence ($E > 1$ Mev) as a Function of Full-Power Service Life	A-3
A-3	San Onofre Unit No. 1 Reactor Coolant System Heatup Limitations Applicable for the First 16 EFPY	A-10
A-4	San Onofre Unit No. 1 Reactor Coolant System Cooldown Limitations Applicable for the First 16 EFPY	A-11

LIST OF TABLES

Table	Title	Page
1-1	End-of-Life Projected Fast Neutron Fluences	1-2
4-1	Chemistry and Heat Treatment of Material Representing the Core Region Shell Plates and Weld Metal From the San Onofre Reactor Vessel	4-3
4-2	Chemistry and Heat Treatment of Surveillance Material Representing 6-Inch-Thick A302B ASTM Correlation Monitor Material	4-4
5-1	Charpy V-Notch Impact Data for San Onofre Pressure Vessel Material Irradiated in Capsule F at 550°F, Fluence 5.14×10^{19} n/cm ² ($E > 1$ Mev)	5-7
5-2	Effect of 550°F Irradiation at 5.14×10^{19} n/cm ² ($E > 1$ Mev) on the Notch Toughness Properties of the San Onofre Reactor Vessel Surveillance Materials	5-9
5-3	Summary of San Onofre Reactor Vessel Surveillance Capsule Charpy Impact Test Results	5-14
5-4	Irradiated Tensile Properties for San Onofre Pressure Vessel Materials	5-16
5-5	Summary of Tensile Results for San Onofre Plate W7601-8 and Weld Metal	5-19
6-1	Neutron Flux Monitors Contained Within Capsule F	6-2
6-2	Irradiation History of Capsule F	6-7
6-3	Spectrum-Averaged Reaction Cross Sections Used in Fast Neutron Flux Derivation	6-11
6-4	Results of Fast Neutron Dosimetry for Capsule F	6-12
6-5	Results of Thermal Neutron Dosimetry for Capsule F	6-13
6-6	Calculated Fast Neutron Flux and Lead Factors for Capsule F	6-15
6-7	Fast Neutron Exposure Derived From Calculated and Measured Results	6-17
A-1	Reactor Vessel Toughness Data (Unirradiated)	A-4

SECTION 1

SUMMARY

The analysis which compared unirradiated with irradiated material properties of the reactor vessel material contained in the third surveillance capsule, designated F, from the Southern California Edison Company San Onofre reactor pressure vessel led to the following conclusions:

- The capsule received an average fast fluence of 5.14×10^{19} n/cm² (E > 1 Mev). The predicted fast fluence for the capsule was 4.92×10^{19} n/cm² (E > 1 Mev).
- The fast fluence of 5.14×10^{19} n/cm² resulted in a 165°F increase in the 50 ft lb reference nil-ductility transition temperature (RT_{NDT}) of the weld metal, which is representative of the most limiting material in the core region of the reactor vessel. The intermediate pressure vessel shell plate W7601-8 exhibited a 50 ft lb transition temperature increase of 110°F (specimens oriented parallel to the rolling direction of the plate). The weld heat-affected-zone material exhibited a 50 ft lb transition temperature increase of 130°F. These transition temperature increases are significantly less than would be predicted using the methods of Regulatory Guide 1.99, and indicate a possible limiting or steady state condition may be occurring.
- An increase of 130°F in the 30 ft lb transition temperature was determined for the ASTM A302B reference correlation monitor material contained in the capsule. The transition temperature increase for the reference material in this capsule and prior capsules is significantly less than predicted from the ASTM trend curve developed for this material and indicates that a limiting or steady state condition has resulted for this material.
- The end-of-life projected fast neutron fluences for the reactor vessel were determined, based on 27 full-power years of operation at 1347 Mw as derived from both calculated and measured surveillance capsule results, and are presented in table 1-1.

TABLE 1-1
END-OF-LIFE PROJECTED FAST NEUTRON FLUENCES

Vessel Location	Fast Neutron Fluence (n/cm ²)	
	Calculated	Measured
Inner surface	1.0 x 10 ²⁰	1.05 x 10 ²⁰
1/4 thickness	4.2 x 10 ¹⁹	4.4 x 10 ¹⁹
3/4 thickness	7.1 x 10 ¹⁸	7.4 x 10 ¹⁸

SECTION 2

INTRODUCTION

This report presents the results of the examination of Capsule F, the third capsule of the continuing surveillance program, which monitors the effects of neutron irradiation on the Southern California Edison Company San Onofre reactor pressure vessel materials under actual operating conditions.

The surveillance program for the San Onofre reactor pressure vessel materials was designed and recommended by the Westinghouse Electric Corporation. A description of the surveillance program and the preirradiation mechanical properties of the reactor vessel materials are presented by Yanichko.^[1] The surveillance program, which was planned to cover the 30-year life of the reactor pressure vessel, was based on ASTM E-185-62.^[2]

Postirradiation data have been obtained from the third material surveillance capsule (Capsule F) removed from San Onofre reactor vessel. This report summarizes the tests and the results, and discusses the analysis of the data.

-
1. Yanichko, S. E., "San Onofre Reactor Vessel Radiation Surveillance Program," WCAP-2834-R1, November 1966.
 2. ASTM Designation E185-62, "Surveillance Tests on Structural Materials in Nuclear Reactors," in ASTM Standards (1962), Part 31, Physical and Mechanical Testing of Metals — Metallography, Nondestructive Testing, Fatigue, Effect of Temperature, Am. Soc. for Testing and Materials, Philadelphia, PA, 1962.

SECTION 3

BACKGROUND

The ability of the large steel pressure vessel containing the reactor core and its primary coolant to resist fracture constitutes an important factor in ensuring safety in the nuclear industry. The beltline region of the reactor pressure vessel is the most critical region of the vessel because it is subjected to significant fast neutron bombardment. The overall effects of fast neutron irradiation on the mechanical properties of low alloy ferritic pressure vessel steels such as SA302 Grade B (base material of the San Onofre reactor pressure vessel beltline) are well-documented in the literature. Generally, low alloy ferritic materials show an increase in hardness and tensile properties and a decrease in ductility and toughness under certain conditions of irradiation.

A method for performing analyses to guard against fast fracture in reactor pressure vessels has been presented in "Protection Against Non-ductile Failure," Appendix G, to Section III of the ASME Boiler and Pressure Vessel Code. The method, utilizing fracture mechanics concepts, is based on the reference nil-ductility temperature, RT_{NDT} .

RT_{NDT} is defined as the greater of the drop weight nil-ductility transition temperature (NDTT per ASTM E-208) or the temperature 60°F less than the 50 ft lb (and 35-mil lateral expansion) temperature as determined from Charpy specimens oriented normal to the rolling direction of the material. The RT_{NDT} of a given material is used to index that material to a reference stress-intensity factor curve (K_{IR} curve) which appears in Appendix G of the ASME Code. The K_{IR} curve is a lower bound of dynamic, crack arrest, and static fracture toughness results obtained from several heats of pressure vessel steel. When a given material is indexed to the K_{IR} curve, allowable stress-intensity factors can be obtained for this material as a function of temperature. Allowable operating limits can then be determined based on these allowable stress-intensity factors.

RT_{NDT} and, in turn, the operating limits of nuclear power plants, can be adjusted to account for the effects of radiation on the reactor vessel material properties. The radiation embrittlement or changes in mechanical properties of a given reactor pressure vessel steel can be monitored by a reactor surveillance program such as the San Onofre reactor vessel radiation surveillance

program,^[1] in which a surveillance capsule is periodically removed from the operating nuclear reactor and the encapsulated specimens are tested. The increase in the Charpy V-notch temperature (ΔRT_{NDT}) due to irradiation is added to the original RT_{NDT} to adjust the RT_{NDT} for radiation embrittlement. This adjusted RT_{NDT} (RT_{NDT} initial + ΔRT_{NDT}) is used to index the material to the K_{IR} curve and, in turn, to set operating limits for the nuclear power plant which take into account the effect of irradiation on the reactor vessel materials.

1. Yanichko, S. E., "San Onofre Reactor Vessel Radiation Surveillance Program," WCAP-2834-R1, November 1966.

SECTION 4

DESCRIPTION OF PROGRAM

Eight surveillance capsules for monitoring the effects of neutron exposure on the San Onofre reactor pressure vessel core region material were inserted in the reactor vessel prior to initial plant startup. The eight capsules were positioned in the reactor vessel between the thermal shield and the vessel wall at locations shown in figure 4-1. The vertical center of the capsules is opposite the vertical center of the core.

Capsule F was removed in December of 1978 after approximately 10 calendar years (7.76 effective full-power years) of plant operation. This capsule contained Charpy V-notch impact, tensile, and WOL specimens (shown in WCAP-2834-R1)^[1] from the intermediate shell ring plates, weld metal representative of the core region of the reactor vessel, and Charpy V-notch specimens from weld heat-affected-zone (HAZ) material. The capsule also contained Charpy V-notch specimens from the 6-inch-thick ASTM correlation monitor material (A302 Grade B) furnished by the U. S. Steel Corporation. The chemistry and heat treatment of the surveillance material is presented in tables 4-1 and 4-2.

All test specimens were machined from the 1/4 thickness location of the plates. Test specimens represent material taken at least one plate thickness from the quenched end of the plate. All base metal Charpy V-notch and tensile specimens were oriented with the longitudinal axis of the specimen parallel to the principal rolling direction of the plates. The WOL test specimens were machined with the simulated crack of the specimen perpendicular to the surfaces and rolling direction of the plates.

Charpy V-notch specimens from the weld metal were oriented with the longitudinal axis of the specimens transverse to the weld direction. Tensile specimens were oriented with the longitudinal axis of the specimen parallel to the weld.

Capsule F contained dosimeter wires of copper, nickel, and aluminum-cobalt (cadmium-shielded and unshielded). In addition, the capsule contained cadmium-shielded dosimeters of Np^{237} and U^{238} , located as shown in figure 4-2.

1. Yanichko, S. E., "San Onofre Reactor Vessel Radiation Surveillance Program," WCAP-2834-R1, November 1966.

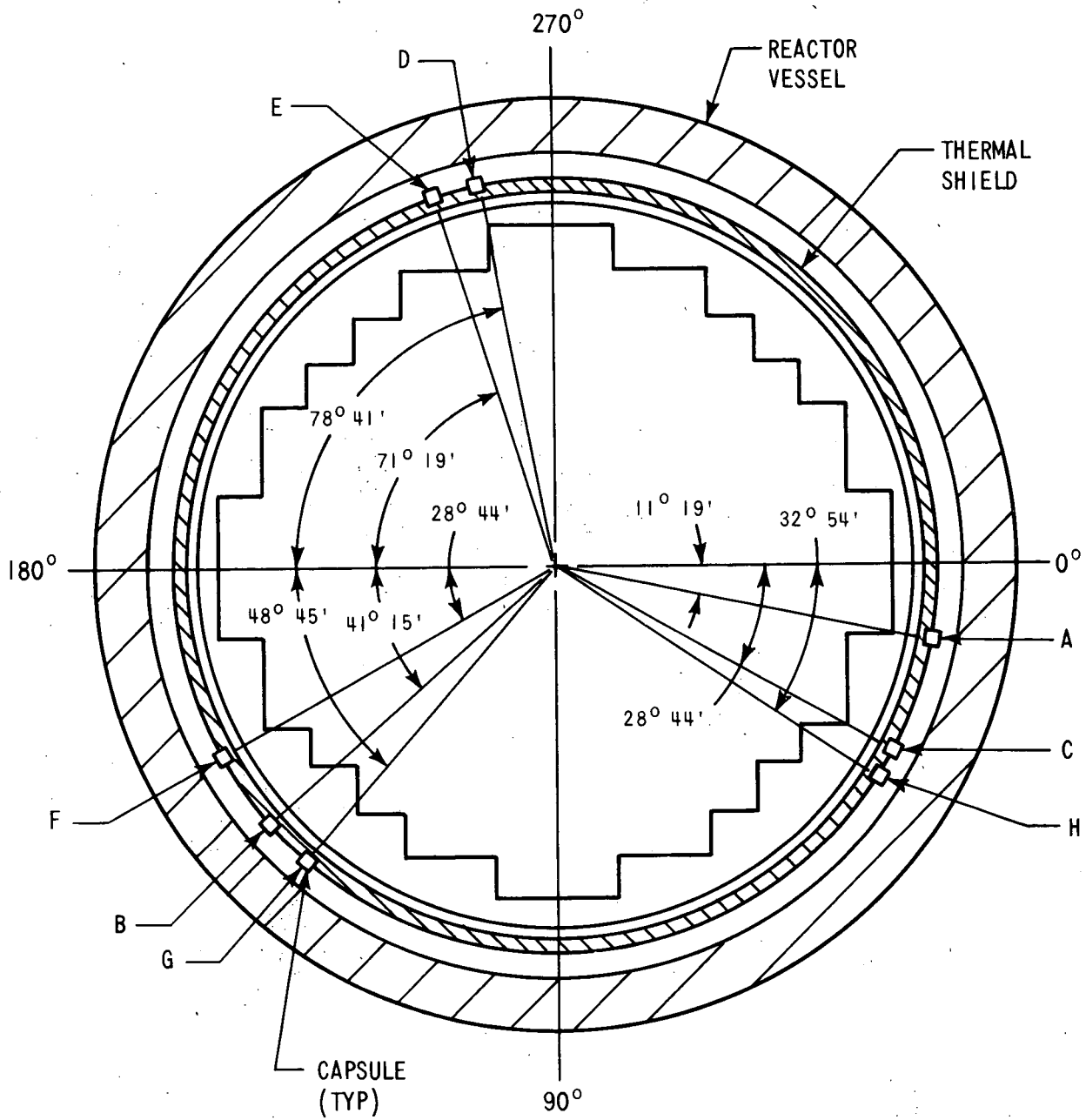


Figure 4-1. Arrangement of Surveillance Capsules in the San Onofre Reactor Vessel

TABLE 4-1

CHEMISTRY AND HEAT TREATMENT OF MATERIAL REPRESENTING THE
CORE REGION SHELL PLATES AND WELD METAL FROM THE
SAN ONOFRE REACTOR VESSEL

Material	Specimen Identification	Data Sources	Chemical Analysis (Percent)							
			C	Mn	Si	P	S	Mo	Cu	V
A302B	W7601-1	SwRI	---	1.45	---	---	---	0.47	0.17	0.02
		Kawin	0.25	1.40	0.30	0.013	0.016	0.43	0.17	0.03
		Lukens	0.22	1.36	0.24	0.013	0.025	0.46	---	---
A302B	W7601-8	SwRI	---	1.39	---	---	---	0.47	0.18	0.02
		Kawin	0.22	1.35	0.26	0.010	0.018	0.47	0.18	0.03
		Lukens	0.20	1.34	0.20	0.012	0.020	0.47	---	---
A302B	W7601-9	SwRI	---	1.50	---	---	---	0.48	0.18	0.02
		Kawin	0.22	1.45	0.26	0.008	0.020	0.45	0.18	0.03
		Lukens	0.19	1.36	0.23	0.014	0.026	0.47	---	---
Weld metal	Specimen ^[a]	SwRI	---	1.26	---	---	---	0.43	0.19	0.04
Weld metal	2461 PC3 ^[b]	Kawin	0.11	1.50	0.35	0.017	0.013	0.47	0.19	0.03

a. Irradiated C_v specimen from Capsule "A".

b. Nozzle cutout.

HEAT TREATMENT

Plate Material	Heated at 1550-1600° — 4 hours — dip quenched Tempered at 1225°F — 4 hours — furnace cooled Stress relieved at 1150°F — 24 hours — furnace cooled
Weld Metal	Stress relieved at 1150°F — 24 hours — furnace cooled

TABLE 4-2
CHEMISTRY AND HEAT TREATMENT OF SURVEILLANCE MATERIAL
REPRESENTING 6-INCH-THICK A302B ASTM CORRELATION
MONITOR MATERIAL

Chemical Analysis (Percent)								
C	Mn	P	S	Mo	Si	Cu	Ni	Cr
0.24	1.34	0.011	0.023	0.51	0.23	0.20	0.18	0.11
HEAT TREATMENT								
<p>The 6-inch-thick plate was charged into a furnace operating at 110°F, heated at a maximum rate of 63°F per hour to 1650°F, held at temperature for 4 hours, and water-quenched to 300°F. The plate was then recharged into a furnace operating at 700° to 750°F, heated at a maximum rate of 63°F per hour to 1200°F, and held at that temperature for 6 hours.</p>								

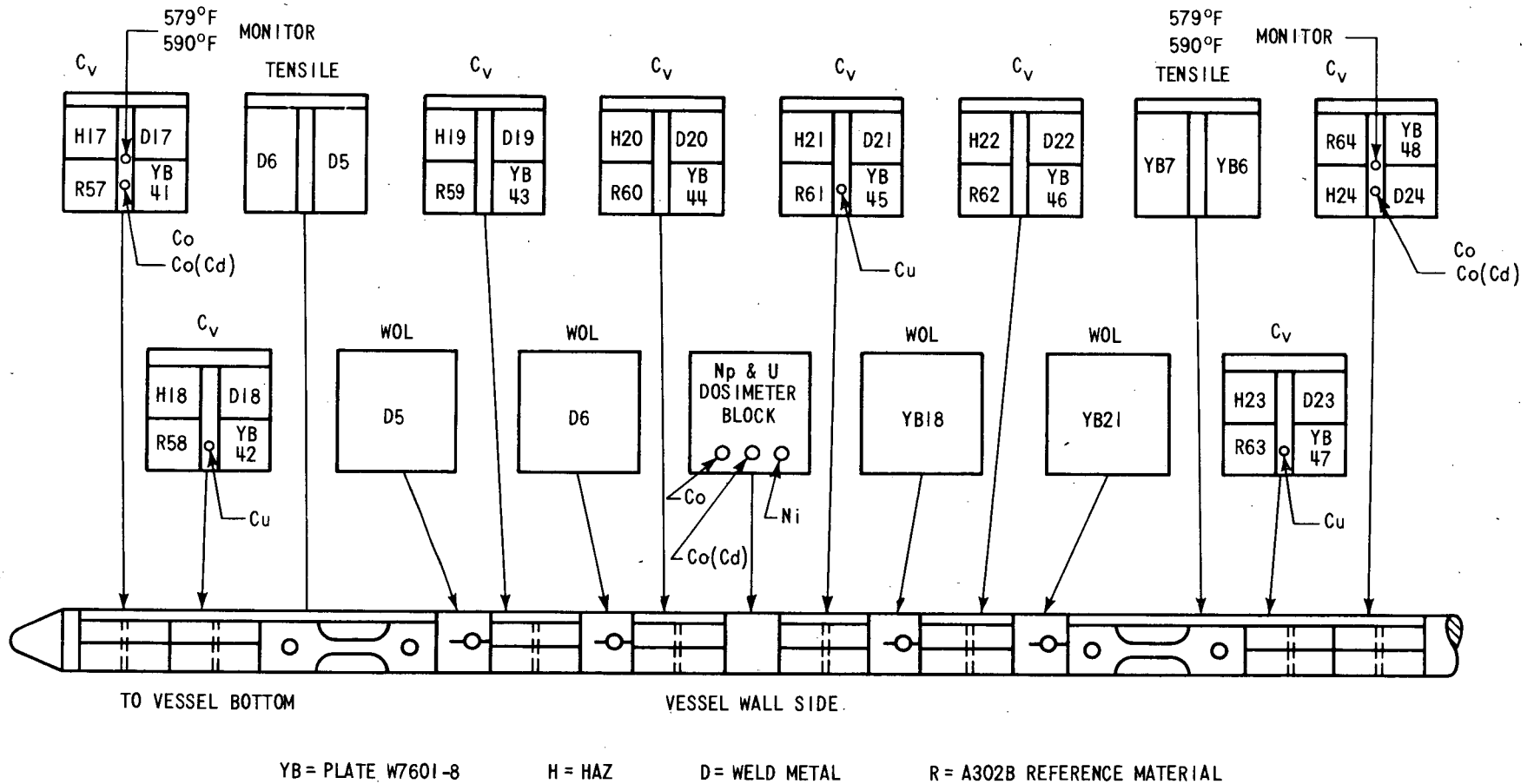


Figure 4-2. Arrangement of Specimens, Thermal Monitors, and Dosimeters in Capsule F

Thermal monitors made from two low melting eutectic alloys and sealed in Pyrex tubes were placed in the capsule, located as shown in figure 4-2. The two eutectic alloys and their melting points are:

2.5% Ag, 97.5% Pb

Melting point 579°F

1.75% Ag, 0.75% Sn, 97.5% Pb

Melting point 590°F

SECTION 5

TESTING OF SPECIMENS FROM CAPSULE F

5-1. TEST PROCEDURE

The postirradiation mechanical testing of the Charpy V-notch and tensile specimens was performed at the Westinghouse Research and Development Laboratory with consultation by Westinghouse Nuclear Energy Systems personnel. Testing was performed in accordance with 10CFR50, Appendices G and H.

Upon receipt of the capsule at the laboratory, the specimens and spacer blocks were carefully removed, inspected for identification number, and checked against the master list in WCAP-2834-R1.^[1] No discrepancies were found.

Examination of the two low-melting (579°F and 590°F) eutectic alloys indicated no melting of either type of thermal monitor. Based on this examination, the maximum temperature to which the test specimens were exposed was less than 579°F.

A Tinius Olsen Model 74 impact test machine was used to test the irradiated Charpy V-notch specimens per ASTM E23-72, "Notched Bar Impact Testing of Metallic Materials." Before initiating tests on the irradiated Charpy-V specimens, the accuracy of the impact machine was checked with a set of standard specimens obtained from the Army Material and Mechanics Research Center in Watertown, Massachusetts. The results of the calibration testing showed that the machine was certified for Charpy V-notch impact testing.

The tensile tests were conducted on a screw-driven Instron testing machine of 20,000 lb capacity per ASTM E8-69, "Tension Testing of Metallic Materials" and ASTM E21-70, "Elevated Temperature Tension Tests of Metallic Materials." The crosshead speed was 0.05 inch per minute. The deformation of the specimen was measured with a strain gage extensometer. The extensometer was calibrated before testing with a Sheffield high magnification drum-type extensometer calibrator.

Elevated-temperature tensile tests were conducted in a split-tube furnace. The specimens were held at temperature a minimum of 20 minutes to stabilize the temperature prior to testing.

1. Yanichko, S. E., "San Onofre Reactor Vessel Radiation Surveillance Program," WCAP-2834-R1, November 1966.

Temperature was monitored with a chromel-alumel thermocouple in contact with the clevis-pin-type upper and lower specimen grips. Temperature was controlled with plus or minus 3°F.

The load-extension data were recorded on the testing machine strip chart. The yield strength, ultimate tensile strength, and uniform elongation were determined from these charts. The reduction in area and total elongation were determined from specimen measurements.

5-2. CHARPY V-NOTCH IMPACT TEST RESULTS

The irradiated Charpy V-notch specimens represented the San Onofre reactor pressure vessel beltline plate material (W7601-8), weld and heat-affected-zone (HAZ) material, and the ASTM reference correlation monitor material. The results are presented in figures 5-1 through 5-4 and table 5-1. Table 5-2 summarizes the increase in the 30 and 50 ft lb energy and 35-mil lateral expansion transition temperature, and the decrease in the upper shelf energy resulting from irradiation to 5.14×10^{19} n/cm².

The test results obtained on shell plate W7601-8 shown in figure 5-1 and table 5-2 resulted in a 30 and 50 ft lb transition temperature increase of 120°F and 110°F, respectively, and a decrease in upper shelf energy of 26 ft lb or 27 percent.

The results of tests on the weld metal are shown in figure 5-2 and table 5-2. These results show that a 145°F and a 165°F transition temperature increase was obtained at the 30 and 50 ft lb levels, respectively. The upper shelf energy decreased 19 ft lb or 19 percent.

Test results for the HAZ material are shown in figure 5-3 and table 5-2. A 30 and 50 ft lb transition temperature increase of 115°F and 130°F, respectively, resulted from irradiation. The upper shelf of the HAZ material decreased 32 ft lb or 30 percent.

Figure 5-4 and table 5-2 present the test results obtained on the ASTM A302B reference correlation monitor material. Respective 30 and 50 ft lb transition temperature increases of 130°F and 135°F were obtained on this material. The upper shelf energy of the correlation monitor material decreased 16 ft lb or 12 percent.

Charpy impact specimen fracture surfaces of the various San Onofre vessel materials and the correlation monitor material are presented in figures 5-5 through 5-8.

Table 5-3 summarizes the Charpy impact test results for first and second capsules^[1,2] and the third capsule removed from the San Onofre reactor to date.

-
1. "Analysis of First Surveillance Material Capsule from San Onofre Unit 1," Southern California Edison Company, July 1971.
 2. Norris, E. B., "Analysis of Second Surveillance Material Capsule from San Onofre Unit 1," SWR1 Project No. 07-2892, June 5, 1972.

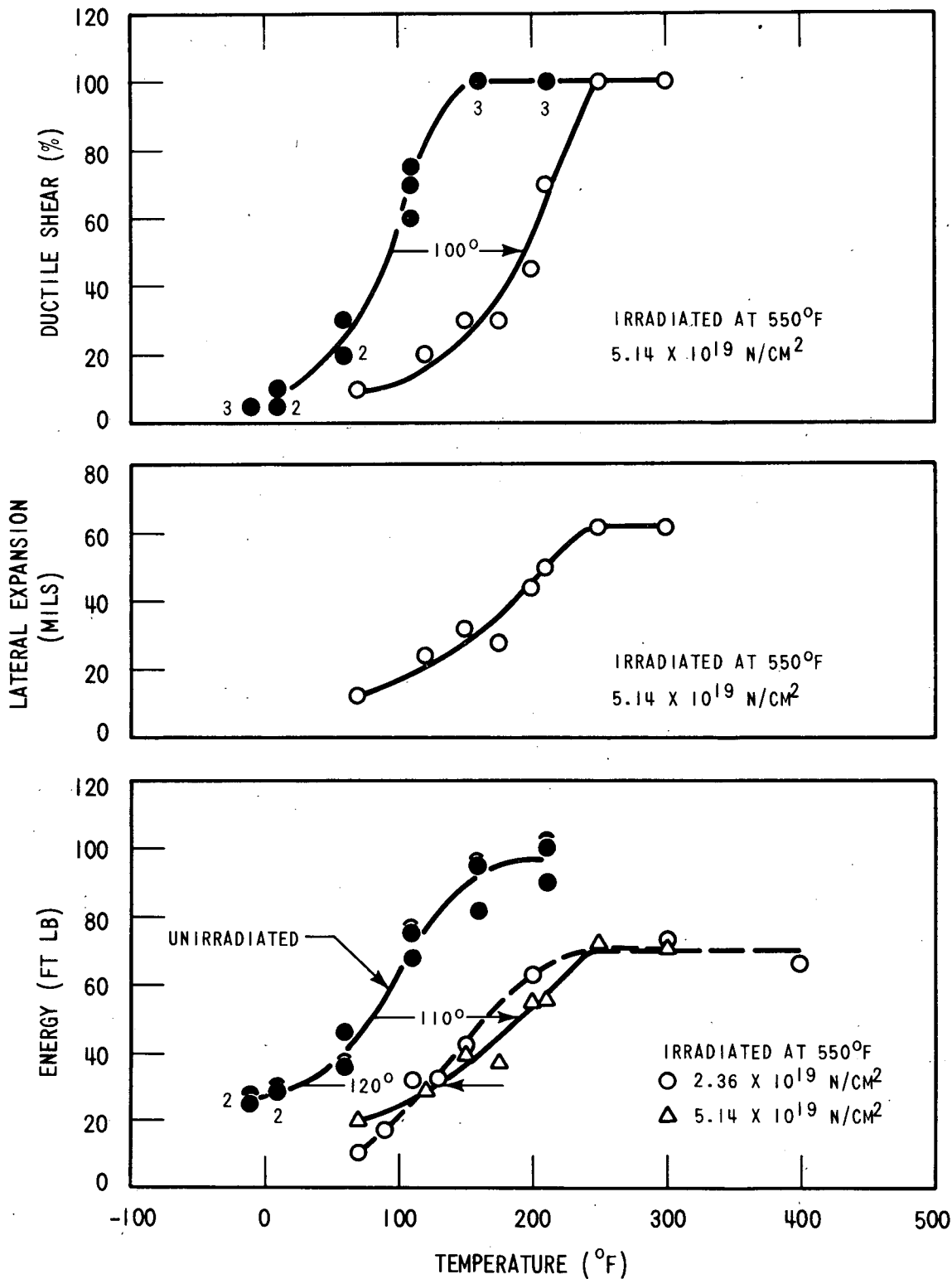


Figure 5-1. Charpy V-Notch Impact Data for San Onofre Pressure Vessel Shell Plate W7601-8

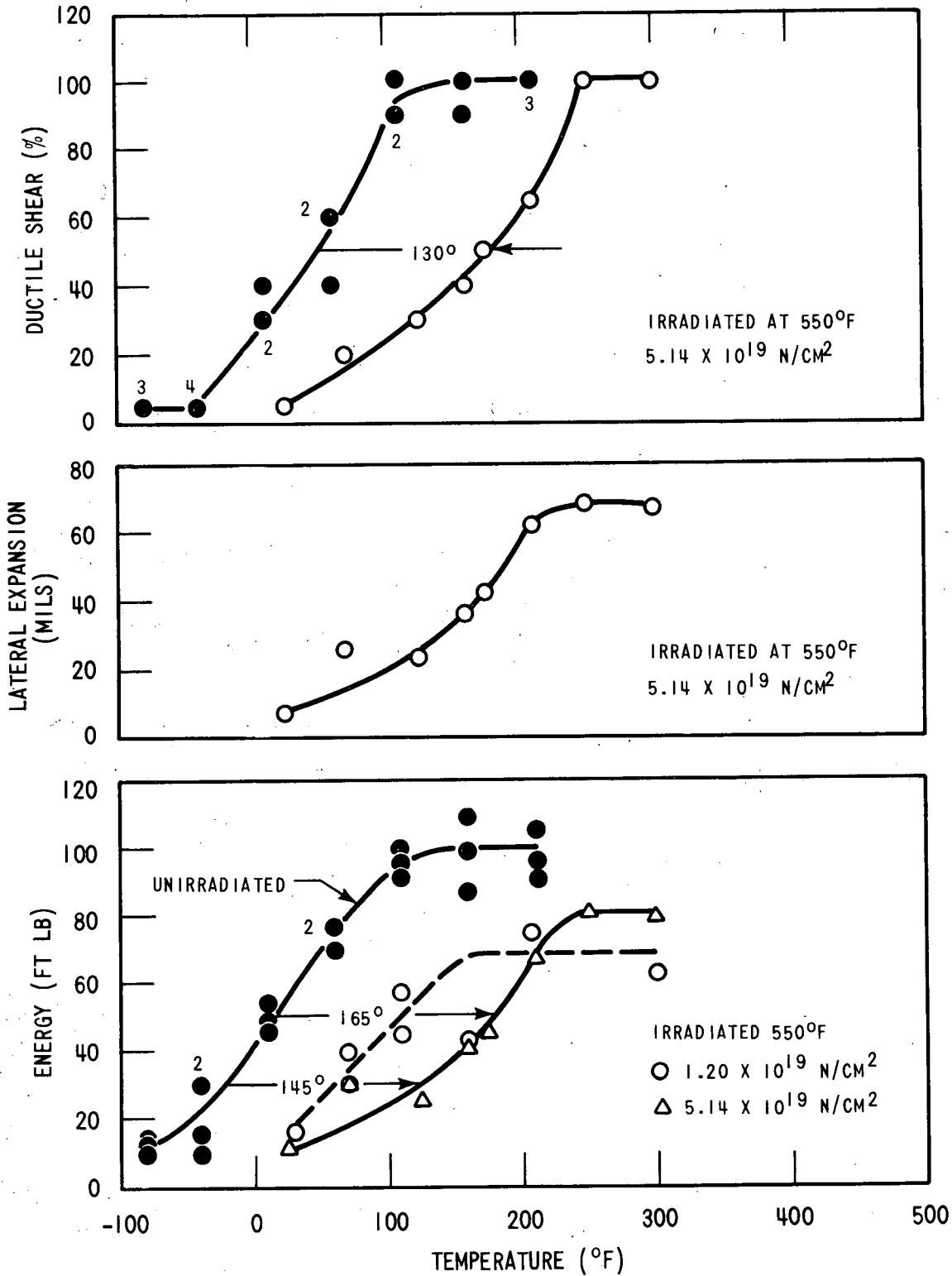


Figure 5-2. Charpy V-Notch Impact Data for San Onofre Pressure Vessel Weld Metal

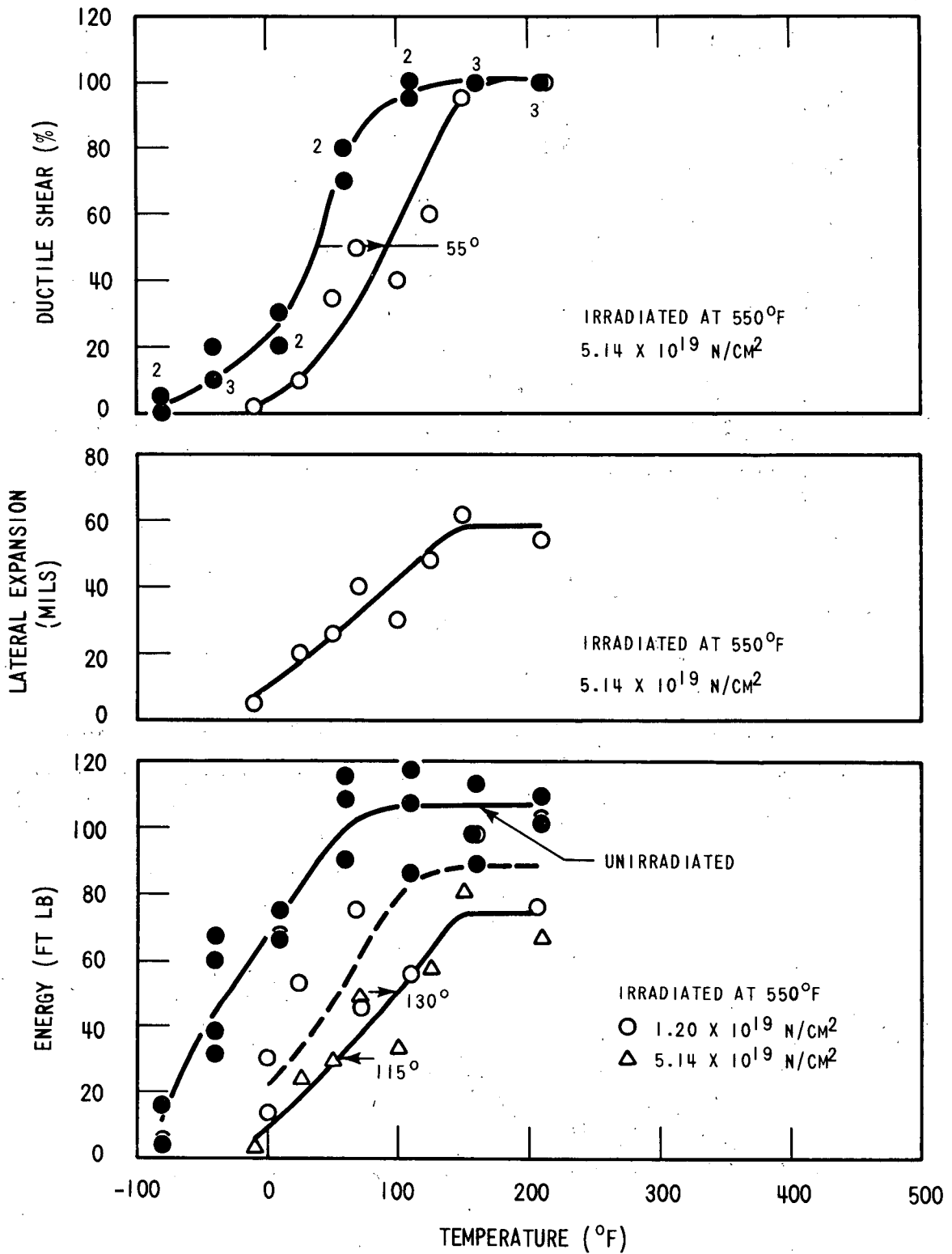


Figure 5-3. Charpy V-Notch Impact Data for San Onofre Pressure Vessel Weld Heat-Affected-Zone Metal

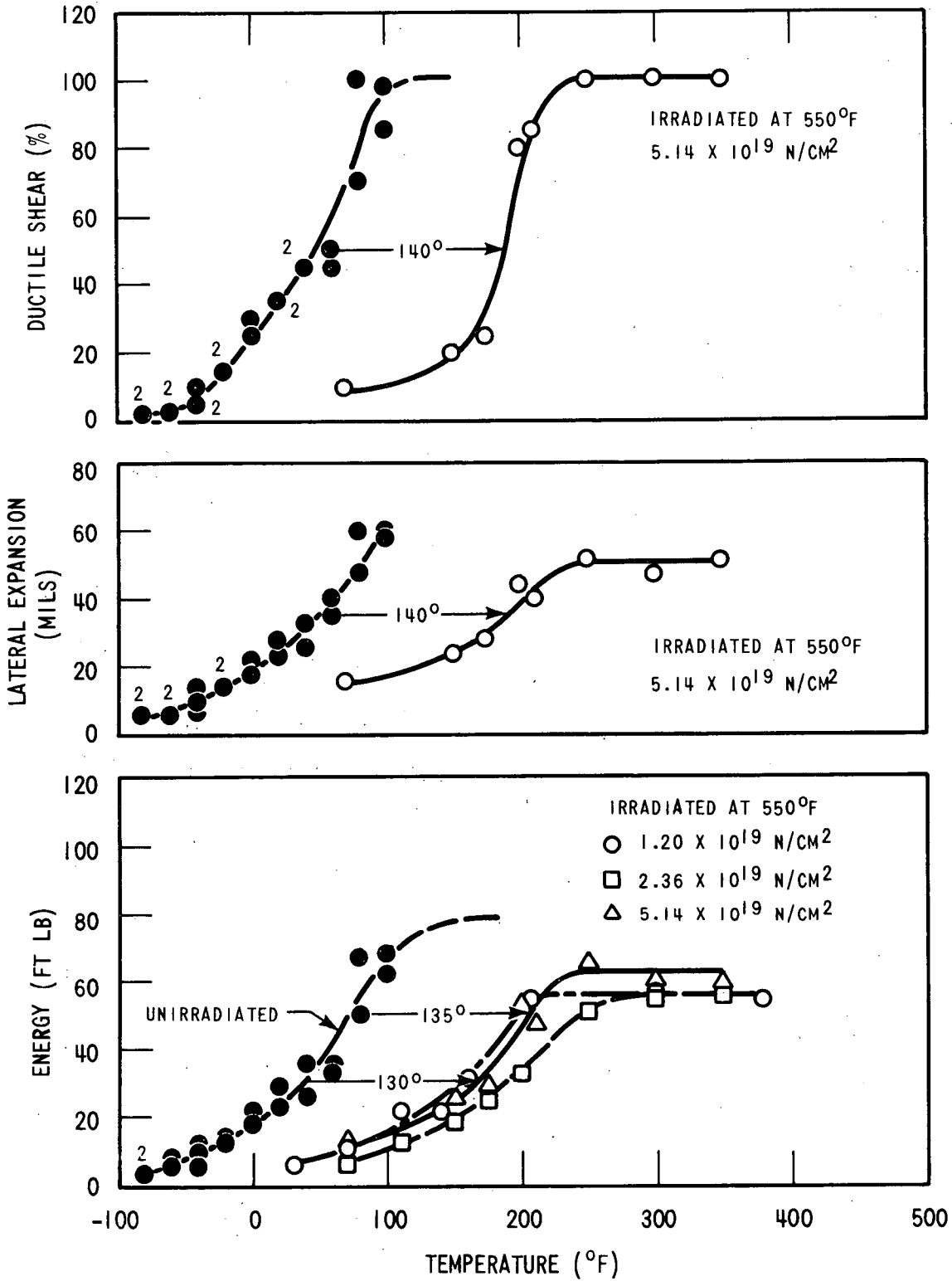


Figure 5-4. Charpy V-Notch Impact Data for A302 Grade B ASTM Correlation Monitor Material

TABLE 5-1
CHARPY V-NOTCH IMPACT DATA FOR SAN ONOFRE PRESSURE VESSEL
MATERIAL IRRADIATED IN CAPSULE F AT 550°F, FLUENCE
 5.14×10^{19} n/cm² (E > 1 Mev)

Material Identification	Specimen Number	Temperature (°F)	Energy (ft lb)	Lateral Expansion (mils)	Shear (%)
W7601-8	YB45	70	20.0	12	10
	YB46	120	29.0	24	20
	YB48	150	40.0	32	30
	YB41	175	37.5	28	30
	YB43	200	55.0	44	45
	YB44	210	56.0	50	70
	YB42	250	72.5	62	100
	YB47	300	71.0	62	100
Weld metal	D19	25	12.0	7	5
	D17	70	30.0	26	20
	D22	125	25.0	23	30
	D23	160	40.0	36	40
	D21	175	45.0	42	50
	D20	210	67.0	62	65
	D18	250	80.0	68	100
	D24	300	79.0	67	100
HAZ metal	H21	-10	3.0	5	2
	H22	25	24.0	20	10
	H20	50	29.5	26	35
	H24	70	49.0	40	50
	H19	100	33.0	30	40
	H18	125	58.0	48	60
	H23	150	81.0	61	95
	H17	210	67.0	54	100

TABLE 5-1 (cont)
CHARPY V-NOTCH IMPACT DATA FOR SAN ONOFRE PRESSURE VESSEL
MATERIAL IRRADIATED IN CAPSULE F AT 550°F, FLUENCE
 5.14×10^{19} n/cm² (E > 1 Mev)

Material Identification	Specimen Number	Temperature (°F)	Energy (ft lb)	Lateral Expansion (mils)	Shear (%)
Correlation monitor	R57	70	12.0	16	10
	R63	150	26.0	24	20
	R58	175	29.0	28	25
	R61	200	53.0	44	80
	R60	212	47.0	40	85
	R62	250	66.0	52	100
	R64	300	60.0	47	100
	R59	350	59.0	51	100

TABLE 5-2
EFFECT OF 550°F IRRADIATION AT 5.14×10^{19} n/cm² (E > 1 Mev) ON THE
NOTCH TOUGHNESS PROPERTIES OF THE SAN ONOFRE REACTOR VESSEL
SURVEILLANCE MATERIALS

Material	Transition Temp (°F)						Δ Temp (°F)			Average Energy Absorption at Full Shear (ft lb)		
	Unirradiated			Irradiated			50 ft lb	30 ft lb	35 mils	Unirradiated	Irradiated	ΔEnergy
	50 ft lb	30 ft lb	35 mils	50 ft lb	30 ft lb	35 mils						
W7601-8	80	10	—	190	130	175	110	120	—	97	71	26
Weld metal	15	-20	—	180	125	160	165	145	—	99	80	19
HAZ metal	-30	-60	—	100	55	80	130	115	—	106	74	32
Correlation material	72	40	50	207	170	190	135	130	140	78	62	16

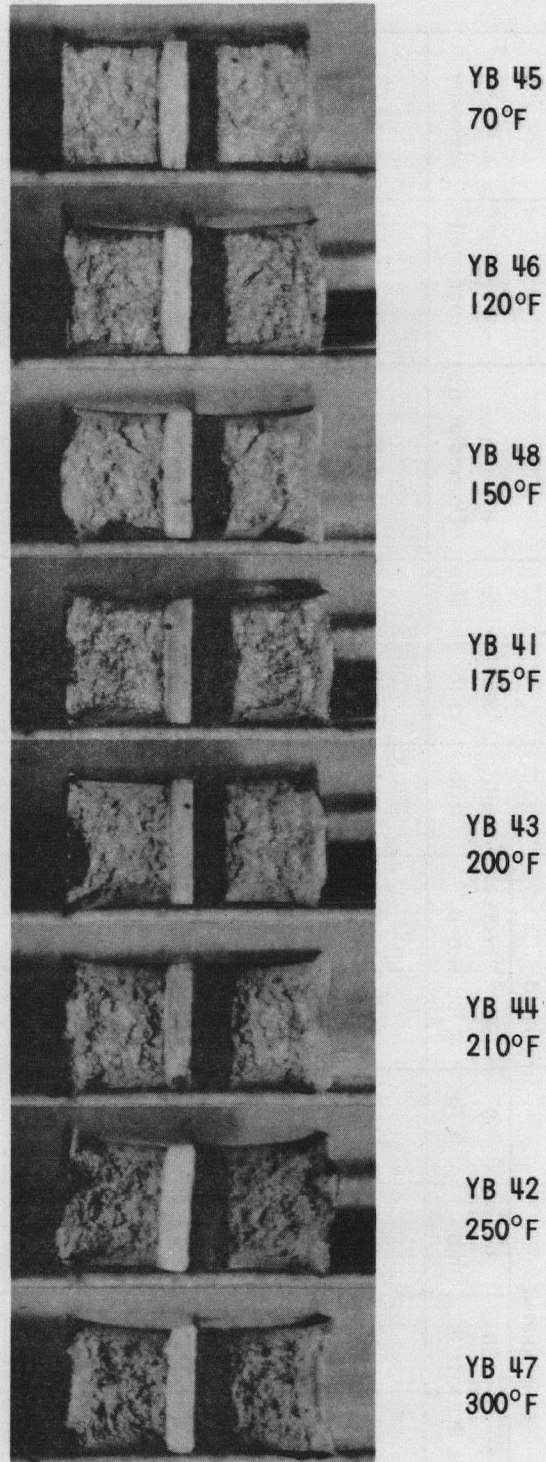


Figure 5-5. Charpy Impact Specimen Fracture Surfaces for San Onofre Pressure Vessel Shell Plate W7601-8

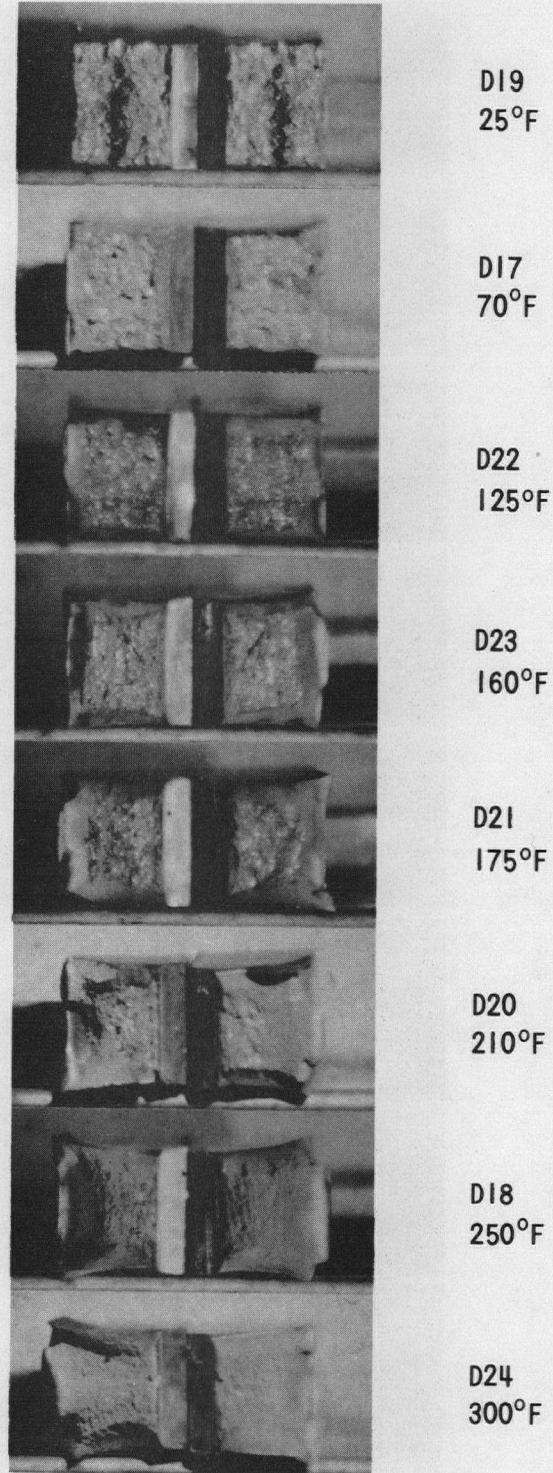


Figure 5-6. Charpy Impact Specimen Fracture Surfaces for San Onofre Weld Metal

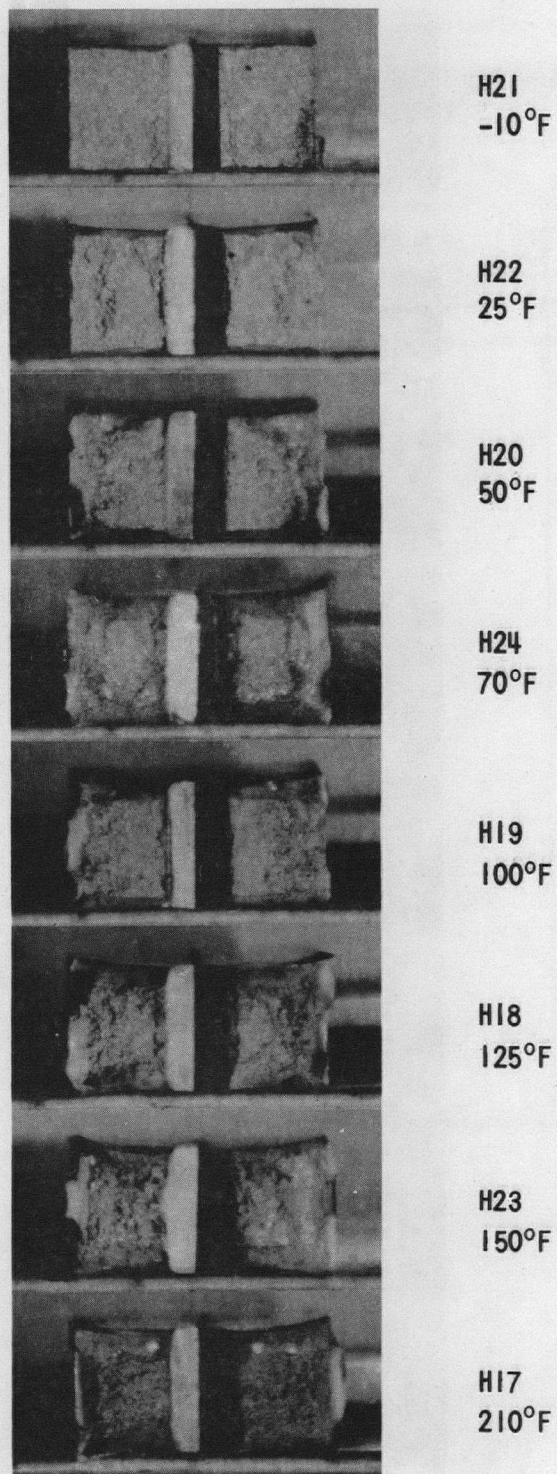


Figure 5-7. Charpy Impact Specimen Fracture Surfaces for San Onofre Weld Heat-Affected-Zone Metal

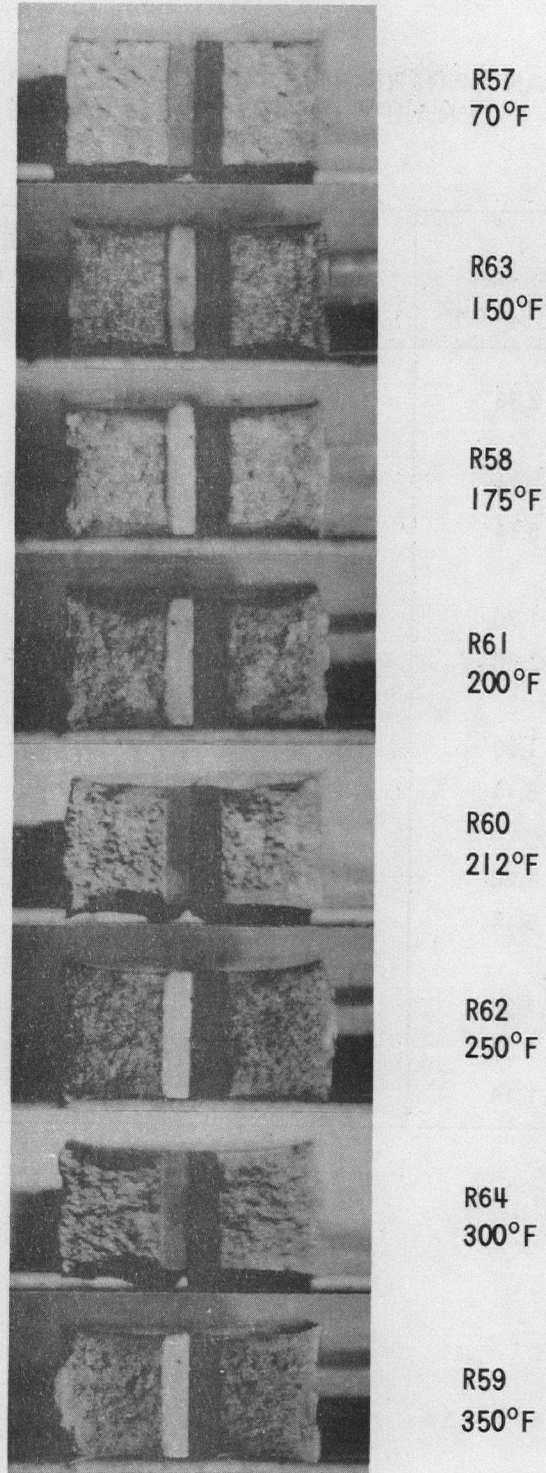


Figure 5-8. Charpy Impact Specimen Fracture Surfaces for A302 Grade B ASTM Correlation Monitor Material

TABLE 5-3
SUMMARY OF SAN ONOFRE REACTOR VESSEL SURVEILLANCE CAPSULE
CHARPY IMPACT TEST RESULTS

Material	Fluence 10 ¹⁹ n/cm ²	30 ft lb Transition Temp Increase (°F)	50 ft lb Transition Temp Increase (°F)	R.G. 1.99 Transition Temp Increase (°F)
W7601-1	2.36	140	110	238
W7601-8	2.36	110	85	246
W7601-8	5.14	120	110	363
W7601-9	1.20	100	85	186
W7601-9	2.36	130	125	261
Weld metal	1.20	80	95	213
Weld metal	5.14	145	165	385
HAZ metal	1.20	80	85	186
HAZ metal	5.14	115	130	385
ASTM correlation monitor	1.20	120	130	192
	2.36	150	175	269
	5.14	130	135	385

The results in table 5-3 show that transition temperature shifts obtained on the San Onofre surveillance materials are considerably less than those which would be predicted from Regulatory Guide 1.99.^[1] The results of tests on the ASTM A302B reference correlation monitor material when compared to the ASTM trend curves^[2] developed for this material also showed lesser transition temperature shifts than predicted. It is suspected that the significantly smaller transition temperature shifts exhibited by the San Onofre surveillance materials resulted from self-annealing during irradiation in the power reactor which tends to create a limiting or steady state condition.

Because the transition temperature increases for the material in the third capsule irradiated to 5.14×10^{19} n/cm² are significantly less than predicted and represent shifts beyond the end of life 1/4 thickness of the vessel (calculated fluence of 4.2×10^{19} n/cm²), normal heatup and cooldown operating limit curves using Westinghouse trend curves for adjusting the reference transition temperature have been prepared. The operating limit curves are considered adequate for continued safe operation of the plant.

5-3. TENSILE TEST RESULTS

Table 5-4 and figures 5-9 and 5-10 give the results of the tensile tests on Plate W7601-8 and weld metal, respectively. A summary of the tests performed to date is presented in table 5-5 which indicates that irradiation to 5.14×10^{19} n/cm² results in no additional increase in yield or tensile strength.

Photographs of the fractured tensile specimens are shown in figures 5-11 and 5-12. A typical stress-strain curve for the tensile tests is shown in figure 5-13.

5-4. WEDGE OPENING LOADING TESTS

Wedge opening loading (WOL) fracture mechanics specimens which were contained in the surveillance capsule have been stored, on the recommendation of the U. S. Nuclear Regulatory Commission, at the Westinghouse Research and Development Center. They will be tested and the results reported at a later date.

-
1. "Effects of Residual Elements on Predicting Radiation Damage to Reactor Vessel Materials," U.S. Nuclear Regulatory Commission Regulatory Guide 1.99, Rev. 1, April 1977.
 2. ASTM DS 54, Radiation Effects Information Generated on the ASTM Reference Correlation Monitor Steels, ASTM, Philadelphia, 1974.

**TABLE 5-4
IRRADIATED TENSILE PROPERTIES FOR SAN ONOFRE PRESSURE VESSEL MATERIALS**

Material Identification	Specimen Number	Test Temp (°F)	0.2% Yield Strength (ksi)	Ultimate Tensile Strength (ksi)	Fracture Strength (ksi)	Fracture Stress (ksi)	Uniform Elong (%)	Total Elong (%)	Reduction In Area (%)
W7601-8	YB6	74	82.1	101.2	74.1	218.0	10.4	23.2	66
W7601-8	YB7	550	71.9	97.1	79.4	153.5	10.7	18.1	48
Weld metal	D6	74	79.6	94.7	65.2	169.3	11.3	25.5	62
Weld metal	D5	550	71.4	90.2	70.3	159.7	9.9	19.8	56

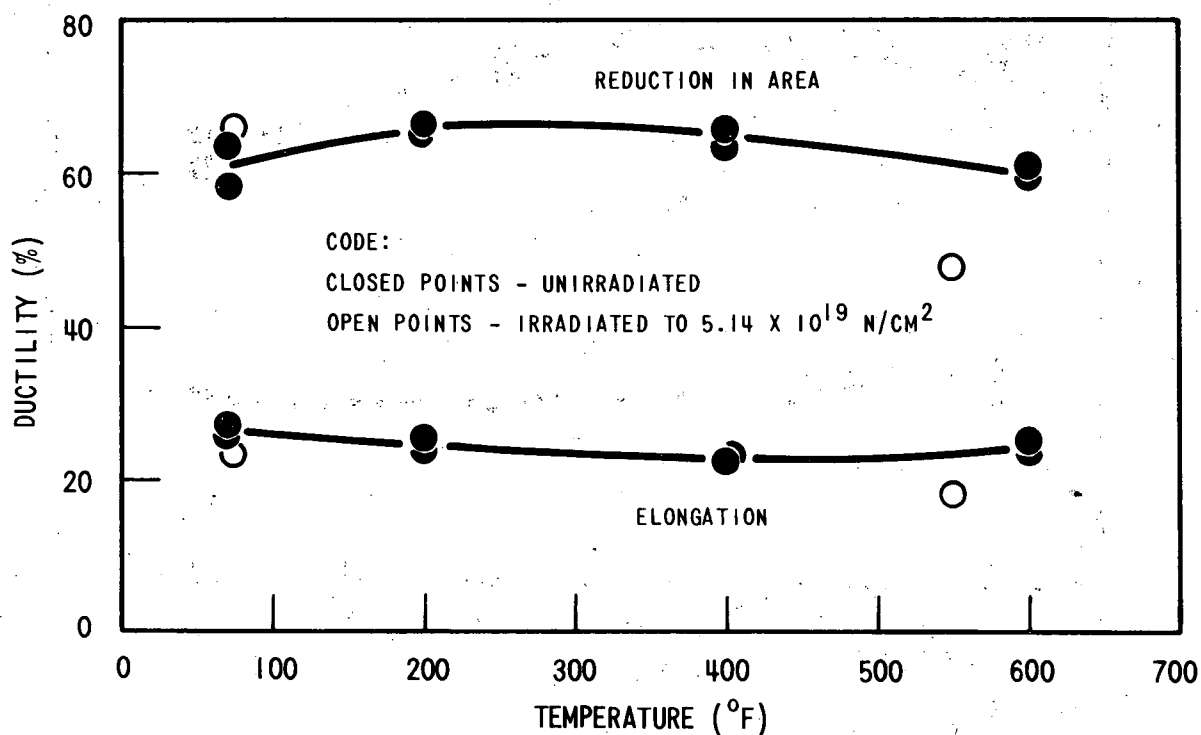
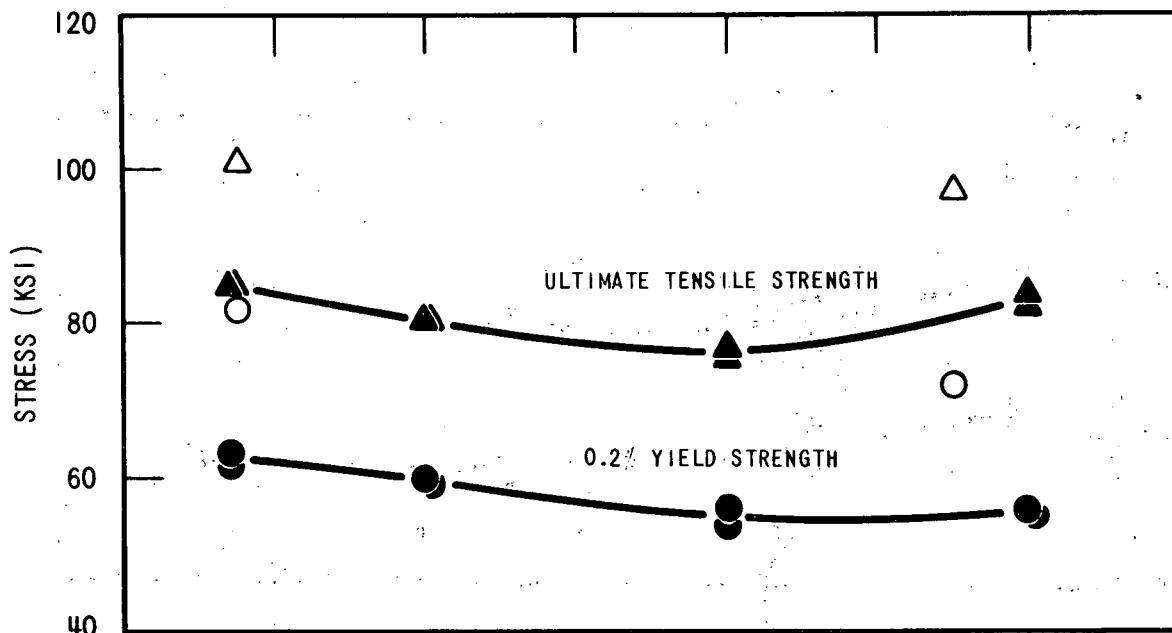


Figure 5-9. Tensile Properties for San Onofre Pressure Vessel Shell Plate W7601-8

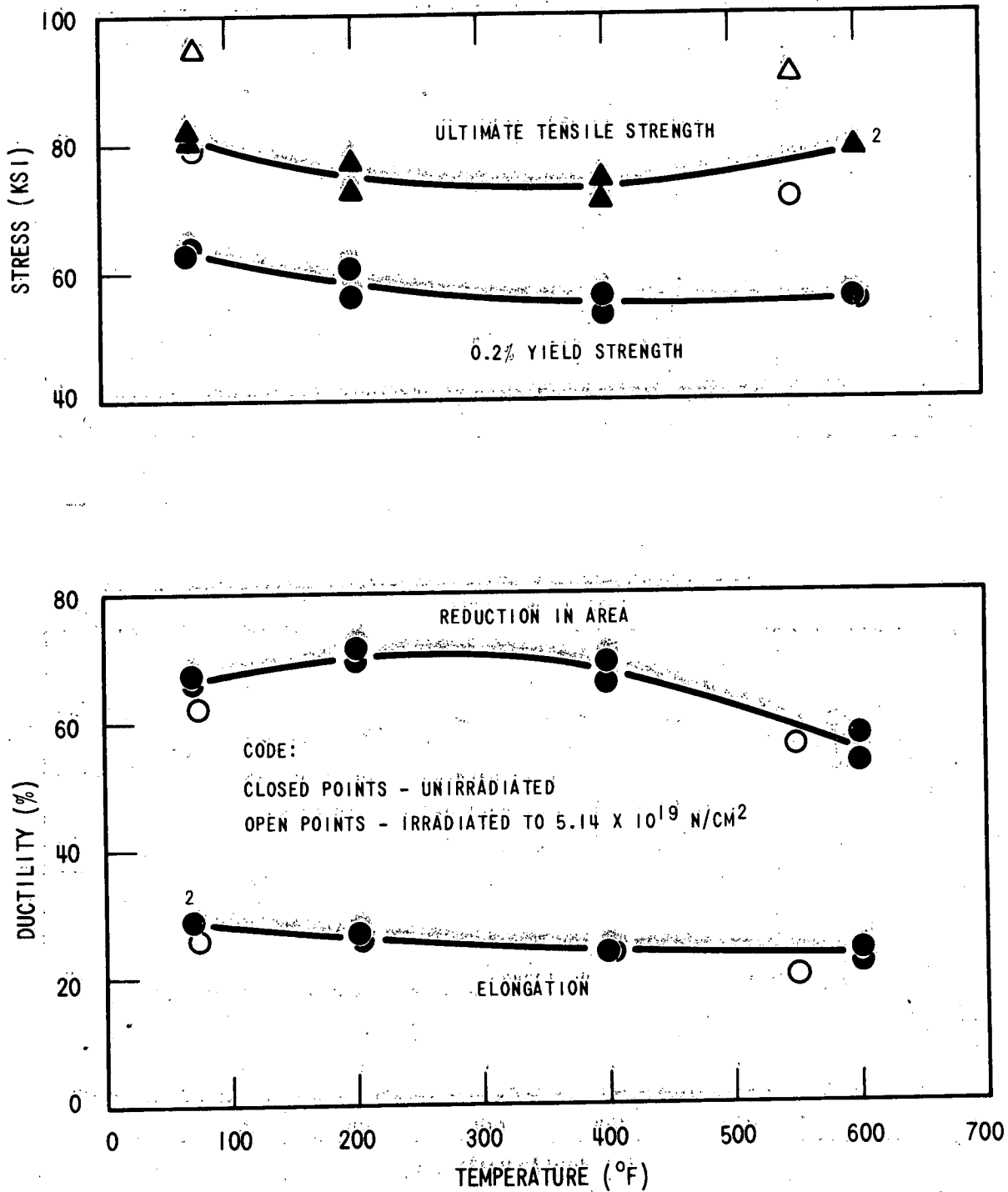
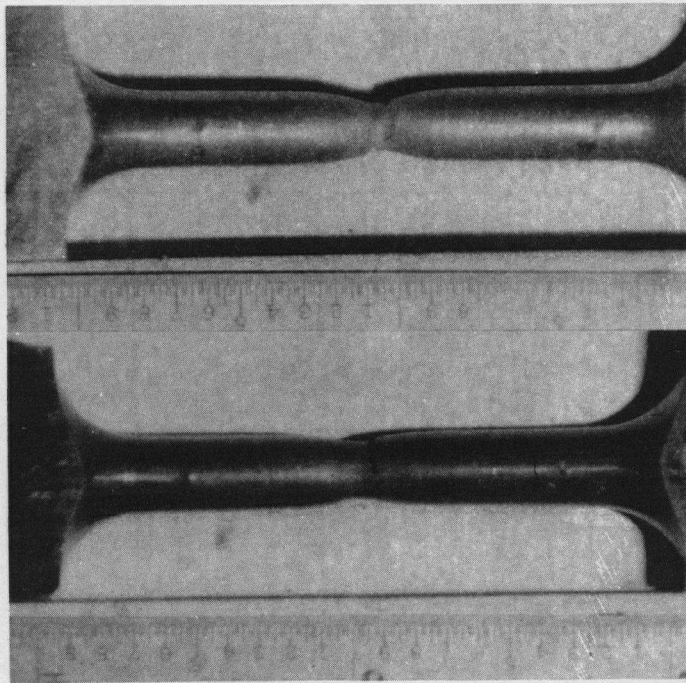


Figure 5-10. Tensile Properties for San Onofre Weld Metal

TABLE 5-5
SUMMARY OF TENSILE RESULTS FOR SAN ONOFRE PLATE W7601-8 AND
WELD METAL

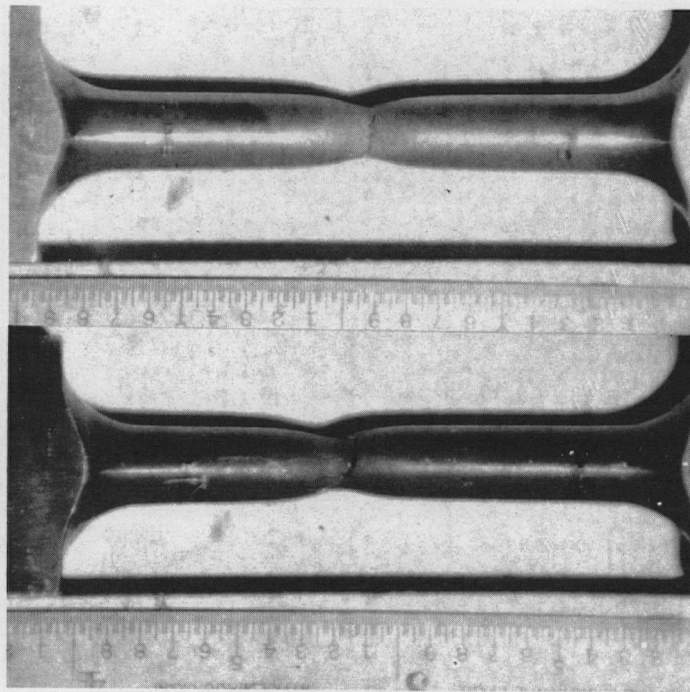
Material Identification	Fluence (n/cm ²)	Test Temp (°F)	0.2% YS (ksi)	UTS (ksi)	RA (%)	Elong (%)
W7601-8	0	room	61.7	84.9	63.4	25.4
W7601-8	0	room	63.3	84.8	58.0	26.9
W7601-8	2.36 x 10 ¹⁹	room	90.1	113.0	63.1	26.0
W7601-8	5.14 x 10 ¹⁹	room	82.1	101.2	66.0	23.2
W7601-8	0	600	55.9	82.3	59.8	24.9
W7601-8	0	600	55.1	83.5	60.8	23.6
W7601-8	5.14 x 10 ¹⁹	550	71.9	97.1	48.0	18.1
Weld metal	0	room	63.7	82.2	66.0	28.6
Weld metal	0	room	63.0	80.8	66.8	28.6
Weld metal	1.20 x 10 ¹⁷	room	83.0	103.2	60.6	28.3
Weld metal	5.14 x 10 ¹⁹	room	79.6	94.7	62.0	25.5
Weld metal	0	600	55.0	78.9	53.2	23.8
Weld metal	0	600	55.6	78.9	57.1	21.8
Weld metal	5.14 x 10 ¹⁹	550	71.4	90.2	56.0	19.8



YB6
74°F

YB7
550°F

Figure 5-11. Fractured Tensile Specimens From San Onofre Shell Plate W7601-8



D6
74°F

D5
550°F

Figure 5-12. Fractured Tensile Specimens From San Onofre Weld Metal

5-22

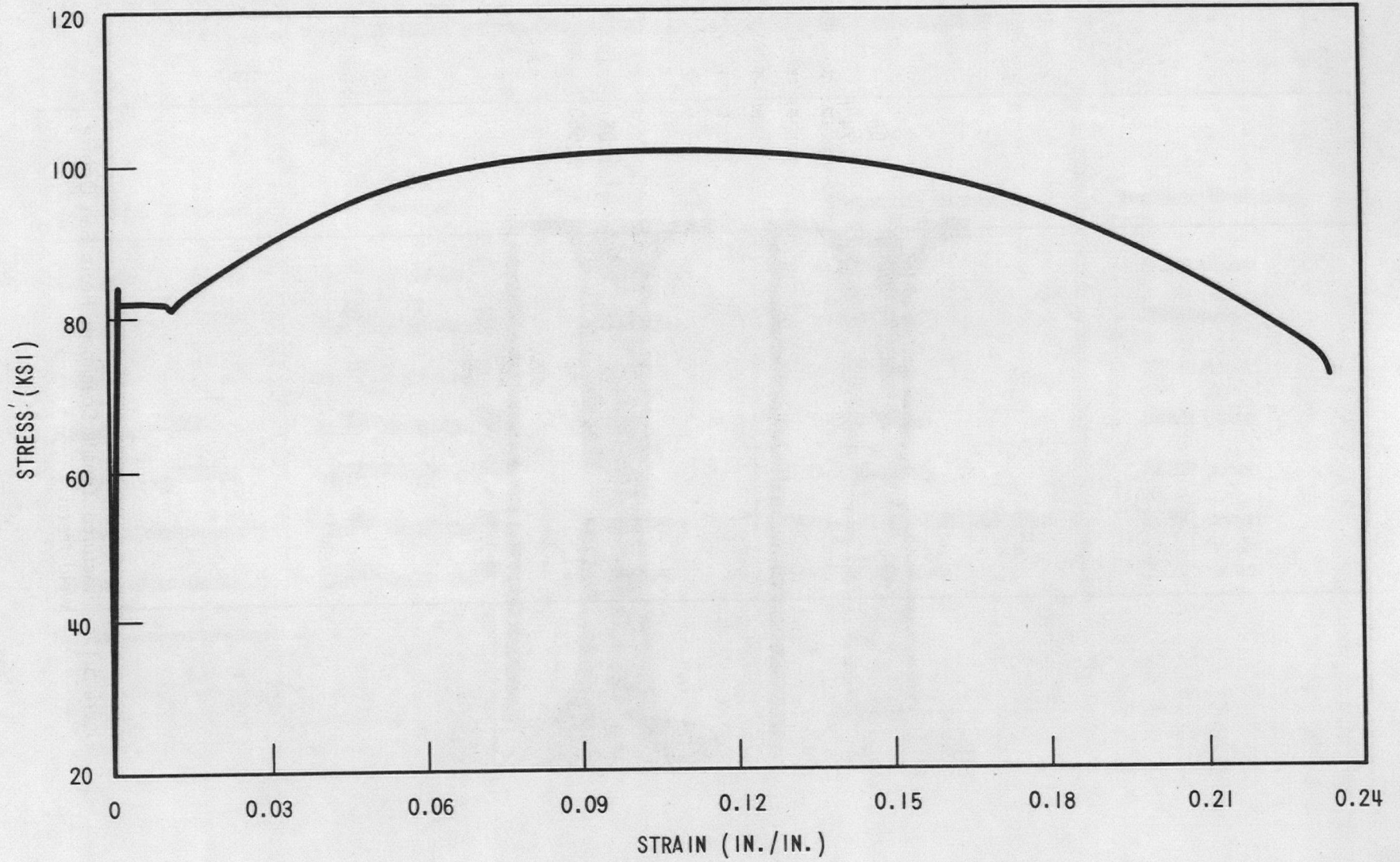


Figure 5-13. Typical Stress-Strain Curve for Tension Specimens
(Tension Specimen No. YB-6)

SECTION 6

NEUTRON DOSIMETRY ANALYSIS

6-1. DESCRIPTION OF NEUTRON FLUX MONITORS

To effect a correlation between neutron exposure and the radiation-induced property changes observed in the test specimens, a number of neutron flux monitors were included as an integral part of the reactor vessel surveillance program. Table 6-1 lists the particular monitors contained within Capsule F along with the nuclear reaction of interest and the energy range of each monitor.

The first five reactions listed in table 6-1 are used as fast neutron monitors to relate neutron fluence ($E > 1.0$ Mev) to the measured shift in RT_{NDT} . To properly account for burnout of the product isotope generated by the fast neutron reactions, it is also necessary to determine the magnitude of the thermal neutron flux at the monitor location. Therefore, bare and cadmium-covered cobalt-aluminum monitors were included within Capsule F.

Figure 4-2 shows the relative locations of the various monitors within Capsule F, and figure 4-1 shows the radial and azimuthal positions of the capsule with respect to the nuclear core, reactor internals, and pressure vessel. The nickel, copper, and cobalt-aluminum monitors (in wire form) were placed in holes drilled in spacers at several axial levels within the capsule. The iron monitors were obtained by drilling samples from selected Charpy test specimens. The cadmium-shielded neptunium and uranium fission monitors were accommodated within the dosimeter block located near the center of the capsule.

The use of activation monitors such as those listed in table 6-1 does not yield a direct measure of the energy-dependent neutron flux level at the point of interest. Rather, the activation process is a measure of the integrated effect that the time and energy-dependent neutron flux has on the target material. An accurate estimate of the average neutron flux level incident on the various monitors may be derived from the activation measurements only if the irradiation parameters are well known. In particular, the following variables are of interest:

- The operating history of the reactor
- The energy response of the monitor

TABLE 6-1
NEUTRON FLUX MONITORS CONTAINED WITHIN CAPSULE F

Monitor Material	Reaction of Interest	Wt% of Target $\frac{\text{gm}_{\text{target}}}{\text{gm}_{\text{monitor}}}$	Response Range	Product Half-Life
Copper	$\text{Cu}^{63} (n,\alpha) \text{Co}^{60}$	0.6917	$E > 4.7 \text{ Mev}$	5.27 years
Iron	$\text{Fe}^{54} (n,p) \text{Mn}^{54}$	0.0585	$E > 1.0 \text{ Mev}$	314 days
Nickel	$\text{Ni}^{58} (n,p) \text{Co}^{58}$	0.6777	$E > 1.0 \text{ Mev}$	71.4 days
Uranium ²³⁸ [a]	$\text{U}^{238} (n,f) \text{Cs}^{137}$	1.0	$E > 0.4 \text{ Mev}$	30.2 years
Neptunium ²³⁷ [a]	$\text{Np}^{237} (n,f) \text{Cs}^{137}$	1.0	$E > 0.08 \text{ Mev}$	30.2 years
Cobalt-Aluminum ^[a]	$\text{Co}^{59} (n,\lambda) \text{Co}^{60}$	0.0015	$0.4 \text{ ev} < E < 0.015 \text{ Mev}$	5.27 years
Cobalt-Aluminum	$\text{Co}^{59} (n,\lambda) \text{Co}^{60}$	0.0015	$E < 0.015 \text{ Mev}$	5.27 years

a. Cadmium shielded monitors

- The neutron energy spectrum at the monitor location
- The physical characteristics of the monitor

6-2. ANALYTICAL PROCEDURES

The analysis of the activation monitors and subsequent derivation of the average neutron flux requires completion of two procedures. First, the disintegration rate of product isotope per unit mass of monitor must be determined. Second, in order to define a suitable spectrum-averaged reaction cross section, the neutron energy spectrum at the monitor location must be calculated.

The energy and spatial distribution of neutron flux within the San Onofre Unit No. 1 reactor geometry was obtained with the DOT^[1] two-dimensional S_n transport code. The radial and azimuthal distributions were obtained from an R, θ computation wherein the reactor core, reactor internals, surveillance capsule, water annuli, pressure vessel, and primary shield concrete were described on the analytical model. These analyses employed 21 neutron energy groups, an S_8 angular quadrature, and a P_1 cross-section expansion. The reactor core power distributions used in the calculations, which were representative of time-averaged conditions over an equilibrium fuel cycle, accounted for rod-by-rod spatial variations in the peripheral fuel assemblies. The analytical geometries described a 45-degree sector of the reactor, assuming one-eighth symmetry. Relative axial variations of neutron flux incident on the reactor vessel were obtained from R, Z DOT calculations based on the equivalent cylindrical core concept.

The specific activity of each of the activation monitors was determined in accordance with established ASTM procedures.^[2,3,4,5,6] Following sample preparation, the activity of each monitor was determined by means of a lithium drifted germanium Ge (Li) gamma spectrometer. The overall standard deviation of the measured data is a function of the precision of sample weighing, the uncertainty in counting, and the acceptable error in detector calibration.

1. Soltesz, R. G., Disney, R. K., Jedruch, J. and Ziegler, S. L., "Nuclear Rocket Shielding Methods, Modification, Updating and Input Data Preparation. Vol. 5 - Two-Dimensional, Discrete Ordinates Transport Technique," WANL-PR(LL)034, Vol. 5, August 1970.
2. ASTM Designation E261-70, "Standard Method for Measuring Neutron Flux by Radioactivation Techniques," in ASTM Standards (1975), Part 45, Nuclear Standards, pp. 745-755, Am Society for Testing and Materials, Philadelphia, Pa. 1975.
3. ASTM Designation E262-70, "Standard Method for Measuring Thermal Neutron Flux by Radioactivation Techniques," in ASTM Standards (1975), Part 45, Nuclear Standards, pp. 756-763, Am. Society for Testing and Materials, Philadelphia, PA. 1975.
4. ASTM Designation E263-70, "Standard Method for Measuring Fast-Neutron Flux by Radioactivation of Iron," in ASTM Standards (1975), Part 45, Nuclear Standards pp. 764-769, Am. Society for Testing and Materials, Philadelphia, PA. 1975.
5. ASTM Designation E481-73T, "Tentative Method of Measuring Neutron - Flux Density by Radioactivation of Cobalt and Silver," in ASTM Standards (1975), Part 45, Nuclear Standards, pp. 887-894, Am. Society for Testing and Materials, Philadelphia, PA. 1975.
6. ASTM Designation E264-70, "Standard Method for Measuring Fast-Neutron Flux by Radioactivation of Nickel," in ASTM Standards (1975), Part 45, Nuclear Standards, pp. 770-774, Am. Society for Testing and Materials, Philadelphia, PA. 1975.

For the samples removed from Capsule F, the overall 2σ deviation in all of the measured data was determined to be plus or minus 10 percent.

Having the measured activity of the monitors and the neutron energy spectrum at the location of interest, the calculation of the fast neutron flux proceeded as follows. The reaction product activity in the monitor was expressed as

$$D = \frac{N_0}{A} f_i \gamma \int_E \sigma(E) \theta(E) \sum_{j=1}^n \frac{P_j}{P_{\max}} (1 - e^{-\lambda\tau_j}) e^{-\lambda\tau_d} \quad (6-1)$$

where

D = induced product activity

N_0 = Avogadro's number

A = atomic weight of the target isotope

f_i = weight fraction of the target isotope in the target material

γ = number of product atoms produced per reaction

$\sigma(E)$ = energy-dependent reaction cross section

$\theta(E)$ = energy-dependent neutron flux at the monitor location with the reactor at full power

P_j = average core power level during irradiation period j

P_{\max} = maximum or reference core power level

λ = decay constant of the product isotope

τ_j = length of irradiation period j

τ_d = decay time following irradiation period j

Because neutron flux distributions were calculated by means of multigroup transport methods and, further, because the prime interest was in the fast neutron flux above 1 Mev, spectrum-averaged reaction cross sections were defined such that the integral term in equation (6-1) could be replaced by the following relation

$$\int_E \sigma(E) \theta(E) = \bar{\sigma} \phi \quad (E > 1 \text{ Mev})$$

where

$$\sigma = \frac{\int_0^{\infty} \sigma(E) \phi(E) dE}{\int_{1.0 \text{ Mev}}^{\infty} \phi(E) dE} = \frac{\sum_{G=1}^n \sigma_g \phi_g}{\sum_{G=G_{1.0 \text{ Mev}}}^n \sigma_g}$$

Thus, equation (6-1) was rewritten

$$D = \frac{N_0}{A} f_i \gamma \bar{\sigma} (E > 1.0 \text{ Mev}) \sum_{j=1}^n \frac{P_j}{P_{\max}} (e^{-\lambda \tau_j}) e^{-\lambda \tau_d}$$

or, solving the neutron flux

$$\phi (E > 1.0 \text{ Mev}) = \frac{D}{\frac{N_0}{A} f_i \gamma \bar{\sigma} \sum_{j=1}^n \frac{P_j}{P_{\max}} (1 - e^{-\lambda \tau_j}) e^{-\lambda \tau_d}} \quad (6-2)$$

The total fluence above 1 Mev was then given by

$$\phi (E > 1.0 \text{ Mev}) = \phi (E > 1.0 \text{ Mev}) \sum_{j=1}^n \frac{P_j}{P_{\max}} \tau_j \quad (6-3)$$

where

$$\sum_{j=1}^n \frac{P_j}{P_{\max}} \tau_j = \text{total effective full power seconds of reactor operation up to the time of capsule removal}$$

An assessment of the thermal neutron flux levels within Capsule F was obtained from the bare and cadmium-covered $\text{Co}^{59} (n, \lambda) \text{Co}^{60}$ data by means of cadmium ratios and the use of a 37-barn 2200 m/sec cross section. Thus,

$$\phi_{\text{th}} = \frac{D_{\text{bare}} \left\{ \frac{R-1}{R} \right\}}{\frac{N_0}{A} f_j \gamma \sigma \sum_{j=1}^n \frac{P_j}{P_{\max}} (1 - e^{-\lambda \tau_j}) e^{-\lambda \tau_d}} \quad (6-4)$$

where

R is defined as $D_{\text{bare}}/D_{\text{Cd-covered}}$

The irradiation history of the flux monitors removed from Capsule F is listed in table 6-2. The spectrum-averaged reaction cross sections derived for each of the fast neutron flux monitors are listed in table 6-3.

6-3. RESULTS OF ANALYSIS

Table 6-4 lists the fast neutron ($E > 1$ Mev) flux and fluence levels derived from the monitors taken from Capsule F. In examining the data listed in table 6-4, it should be noted that the Fe^{54} monitors were positioned within the surveillance capsule at a radius of 168.68 and 169.68 cm relative to the core centerline. The corresponding radius of the U^{238} and Np^{237} monitors was 168.91 cm and that of the Ni^{58} and Cu^{63} monitors was 169.68 cm. Thus, it should be expected that the measured neutron flux levels reflect the flux gradient caused by attenuation within the test specimens. Table 6-5 summarizes the thermal neutron flux obtained from the cobalt-aluminum monitors. Due to the relatively low thermal neutron flux at the capsule location, no burnup correction was made to any of the measured activities. The maximum error introduced by this assumption is estimated to be less than 1 percent of the Ni^{58} (n, p) Co^{58} reaction and even less significant for all the other fast reactions.

Figures 6-1 through 6-3 and table 6-6 summarize results of the S_n transport calculations for the San Onofre reactor vessel. In figure 6-1, the calculated maximum fast neutron flux levels at the pressure vessel inner radius, 1/4 thickness location, and 3/4 thickness location are presented as a function of azimuthal angle. Figure 6-2 shows the relative axial variation of neutron flux. Absolute axial variations of fast neutron flux may be obtained by multiplying the levels given in figure 6-1 by the appropriate values from figure 6-2. In figure 6-3, the calculated maximum end-of-life fast neutron exposure of the San Onofre reactor vessel is given as a function of radial position within the vessel wall. Table 6-6 lists the calculated fast neutron flux levels interior to Capsule F along with the lead factors (LF) relating capsule exposure to vessel exposure. The lead factor is defined as the ratio of the calculated flux at the monitor location to the calculated peak neutron flux incident on the reactor vessel.

Based on the iron data in table 6-4, the average fast neutron fluence incident on the front row of Charpy specimens is determined to be 5.74×10^{19} n/cm², while that on the back row of the specimens is 4.53×10^{19} n/cm² or an average value of 5.14×10^{19} n/cm². These measured values correspond to analytical values of 5.54×10^{19} and 4.29×10^{19} n/cm², respectively, or an average value of 4.91×10^{19} n/cm². A comparison of these values shows excellent agreement.

TABLE 6-2
IRRADIATION HISTORY OF CAPSULE F

Month	P _{avg} (Mw)	P _{max} (Mw)	P _{avg} /P _{max}	Irradiation Time (days)	Decay ^[a] Time (days)
6/67-12/67	240	1347	0.178	201	4028
1/68	944	1347	0.701	31	3997
2/68	700	1347	0.520	29	3968
3/68	277	1347	0.206	31	3937
4/68-8/68	0	1347	0.000	153	3784
9/68	254	1347	0.189	30	3754
10/68	1135	1347	0.842	31	3723
11/68	1182	1347	0.877	30	3693
12/68	1077	1347	0.799	31	3662
1/69	852	1347	0.632	31	3631
2/69	1150	1347	0.854	28	3603
3/69	773	1347	0.574	31	3572
4/69	1034	1347	0.768	30	3542
5/69	1210	1347	0.898	31	3511
6/69	789	1347	0.592	30	3481
7/69	0	1347	0.000	31	3450
8/69	587	1347	0.436	31	3419
9/69	1342	1347	0.997	30	3389
10/69	919	1347	0.682	31	3358
11/69	1331	1347	0.988	30	3328
12/69	1329	1347	0.986	31	3297
1/70-7/70	1253	1347	0.930	212	3085
8/70	1325	1347	0.984	31	3054
9/70	1337	1347	0.993	30	3024
10/70	80	1347	0.059	31	2993
11/70	299	1347	0.222	30	2963
12/70	1342	1347	0.996	31	2932

a. Decay time is referenced to the counting date of the Fe, Ni, Cu, and Co monitors (1/10/79). The Np and U monitors were counted on 1/19/79.

TABLE 6-2 (cont)
IRRADIATION HISTORY OF CAPSULE F

Month	P_{avg} (Mw)	P_{max} (Mw)	P_{avg}/P_{max}	Irradiation Time (days)	Decay ^[a] Time (days)
1/71	1328	1347	0.986	31	2901
2/71	1328	1347	0.986	28	2873
3/71	1330	1347	0.987	31	2842
4/71	1317	1347	0.978	30	2812
5/71	934	1347	0.694	31	2781
6/71	1138	1347	0.845	30	2751
7/71	980	1347	0.727	31	2720
8/71	1124	1347	0.835	31	2689
9/71	1252	1347	0.930	30	2659
10/71	1079	1347	0.801	31	2628
11/71	1115	1347	0.828	30	2598
12/71	1024	1347	0.760	31	2567
1/72	0	1347	0.000	31	2536
2/72	181	1347	0.134	29	2507
3/72	1272	1347	0.944	31	2476
4/72	1237	1347	0.919	30	2446
5/72	1019	1347	0.756	31	2415
6/72	1307	1347	0.970	30	2385
7/72	910	1347	0.676	31	2354
8/72	1190	1347	0.884	31	2323
9/72	1165	1347	0.865	30	2293
10/72	1051	1347	0.780	31	2262
11/72	1327	1347	0.985	30	2232
12/72	1342	1347	0.996	31	2201
1/73	1115	1347	0.828	31	2170
2/73	1326	1347	0.984	28	2142
3/73	1340	1347	0.995	31	2111
4/73	1322	1347	0.981	30	2081

a. Decay time is referenced to the counting date of the Fe, Ni, Cu, and Co monitors (1/10/79). The Np and U monitors were counted on 1/19/79.

TABLE 6-2 (cont)
IRRADIATION HISTORY OF CAPSULE F

Month	P_{avg} (Mw)	P_{max} (Mw)	P_{avg}/P_{max}	Irradiation Time (days)	Decay ^[a] Time (days)
5/73	1333	1347	0.989	31	2050
6/73	43	1347	0.032	30	2020
7/73	121	1347	0.090	31	1989
8/73	1103	1347	0.819	31	1958
9/73	1312	1347	0.974	30	1928
10/73	845	1347	0.627	31	1897
11/73-12/73	0	1347	0.000	61	1836
1/74	369	1347	0.274	31	1805
2/74	1347	1347	1.000	28	1777
3/74	1306	1347	0.970	31	1746
4/74	1182	1347	0.878	30	1716
5/74	471	1347	0.349	31	1685
6/74	1315	1347	0.976	30	1655
7/74	1180	1347	0.876	31	1624
8/74	1330	1347	0.987	31	1593
9/74	1237	1347	0.919	30	1563
10/74	1193	1347	0.885	31	1532
11/74	1330	1347	0.987	30	1502
12/74	1347	1347	1.000	31	1471
1/75	1330	1347	0.987	31	1440
2/75	1334	1347	0.990	28	1409
3/75	579	1347	0.430	31	1381
4/75	277	1347	0.206	30	1351
5/75	1304	1347	0.968	31	1320
6/75	1090	1347	0.809	30	1290
7/75	1347	1347	1.000	31	1259
8/75	1337	1347	0.993	31	1228
9/75	1347	1347	1.000	30	1198

a. Decay time is referenced to the counting date of the Fe, Ni, Cu, and Co monitors (1/10/79). The Np and U monitors were counted on 1/19/79.

TABLE 6-2 (cont)
IRRADIATION HISTORY OF CAPSULE F

Month	P _{avg} (Mw)	P _{max} (Mw)	P _{avg} /P _{max}	Irradiation Time (days)	Decay ^[a] Time (days)
10/75	1320	1347	0.980	31	1167
11/75	1347	1347	1.000	30	1137
12/75	1347	1347	1.000	31	1106
1/76	1311	1347	0.973	31	1075
2/76	1306	1347	0.969	29	1046
3/76	1337	1347	0.993	31	1015
4/76	913	1347	0.678	30	985
5/76	1342	1347	0.996	31	954
6/76	1315	1347	0.976	30	924
7/76	1144	1347	0.849	31	893
8/76	1089	1347	0.808	31	862
9/76	930	1347	0.691	30	832
10/76-12/76	0	1347	0.000	92	740
1/77-3/77	0	1347	0.000	90	650
4/77	669	1347	0.496	30	620
5/77	1340	1347	0.995	31	589
6/77	1332	1347	0.989	30	559
7/77	1335	1347	0.991	31	528
8/77	1313	1347	0.975	31	497
9/77	374	1347	0.278	30	467
10/77	1040	1347	0.772	31	436
11/77	1285	1347	0.954	30	406
12/77	1340	1347	0.995	31	375
1/78	1347	1347	1.000	31	344
2/78	1347	1347	1.000	28	316
3/78	1337	1347	0.993	31	285
4/78	459	1347	0.341	30	255

a. Decay time is referenced to the counting date of the Fe, Ni, Cu, and Co monitors (1/10/79). The Np and U monitors were counted on 1/19/79.

TABLE 6-2 (cont)
IRRADIATION HISTORY OF CAPSULE F

Month	P _{avg} (Mw)	P _{max} (Mw)	P _{avg} /P _{max}	Irradiation Time (days)	Decay ^[a] Time (days)
5/78	920	1347	0.683	31	224
6/78	896	1347	0.665	30	194
7/78	1164	1347	0.864	31	163
8/78	1238	1347	0.919	31	132
9/78	1033	1347	0.767	15	117

a. Decay time is referenced to the counting date of the Fe, Ni, Cu, and Co monitors (1/10/79). The Np and U monitors were counted on 1/19/79.

TABLE 6-3
SPECTRUM AVERAGED REACTION CROSS SECTIONS USED IN
FAST NEUTRON FLUX DERIVATION

Reaction	$\bar{\sigma}$ (barns)
Fe ⁵⁴ (n,p) Mn ⁵⁴	0.0664
Ni ⁵⁸ (n,p) Co ⁵⁸	0.0891
Cu ⁶³ (n, α) Co ⁶⁰	0.000472
U ²³⁸ (n,f) F.P.	0.343
Np ²³⁷ (n,f) F.P.	2.80

TABLE 6-4
RESULTS OF FAST NEUTRON DOSIMETRY FOR CAPSULE F

Reaction and Monitor Location	Measured ^[a] Activity (dps/gm)	ϕ (E > 1.0 Mev) ^[b] (n/cm ² -sec)	Φ (E > 1.0 Mev) ^[b] (n/cm ²)
Fe⁵⁴ (n,p) Mn⁵⁴			
Core Side Charpy			
D-17	5.86 x 10 ⁶	2.37 x 10 ¹¹	5.81 x 10 ¹⁹
D-20	6.20 x 10 ⁶	2.51 x 10 ¹¹	6.15 x 10 ¹⁹
D-24	5.30 x 10 ⁶	2.15 x 10 ¹¹	5.27 x 10 ¹⁹
Vessel Side Charpy			
R-57	4.57 x 10 ⁶	1.85 x 10 ¹¹	4.53 x 10 ¹⁹
R-60	4.85 x 10 ⁶	1.96 x 10 ¹¹	4.80 x 10 ¹⁹
R-64	4.30 x 10 ⁶	1.74 x 10 ¹¹	4.26 x 10 ¹⁹
Ni⁵⁸ (n,p) Co⁵⁸			
Center	2.18 x 10 ⁷	1.36 x 10 ¹¹	3.33 x 10 ¹⁹
Cu⁶³ (n,α) Co⁶⁰			
Top	3.40 x 10 ⁵	2.06 x 10 ¹¹	5.05 x 10 ¹⁹
Center	3.64 x 10 ⁵	2.21 x 10 ¹¹	5.41 x 10 ¹⁹
Bottom	3.69 x 10 ⁵	2.24 x 10 ¹¹	5.49 x 10 ¹⁹
Np²³⁷ (n,f) Cs¹³⁷			
Center	8.32 x 10 ⁶	1.25 x 10 ¹¹	3.06 x 10 ¹⁹
U²³⁸ (n,f) Cs¹³⁷			
Center	1.96 x 10 ⁶	2.29 x 10 ¹¹	5.61 x 10 ¹⁹

a. Mn⁵⁴, Co⁵⁸, and Co⁶⁰ activities are referenced to 1/10/79. Cs¹³⁷ activities are referenced to 1/19/79.
 b. Derived flux and fluence levels are subject to ± 10 percent measurement uncertainty.

TABLE 6-5
RESULTS OF THERMAL NEUTRON DOSIMETRY FOR CAPSULE F

Monitor Location	BARE ^[a] Activity (dps/gm)	Cd Covered Activity ^[a] (dps/gm)	ϕ_{th} ^[b] (n/cm ² -sec)
Center	5.52×10^7	3.11×10^7	8.08×10^{10}

a. Co⁶⁰ activities are referenced to 1/10/79.

b. Derived flux level is subject to ± 10 percent measurement error.

TABLE 6-6
CALCULATED FAST NEUTRON FLUX AND LEAD FACTORS
FOR CAPSULE F

Location Within Capsule F	ϕ (E > 1.0 Mev) (n/cm ² -sec)	Lead Factor
Core Side Charpy	2.26×10^{11}	1.93
Dosimeter Block	2.11×10^{11}	1.80
Vessel Side Charpy	1.75×10^{11}	1.50

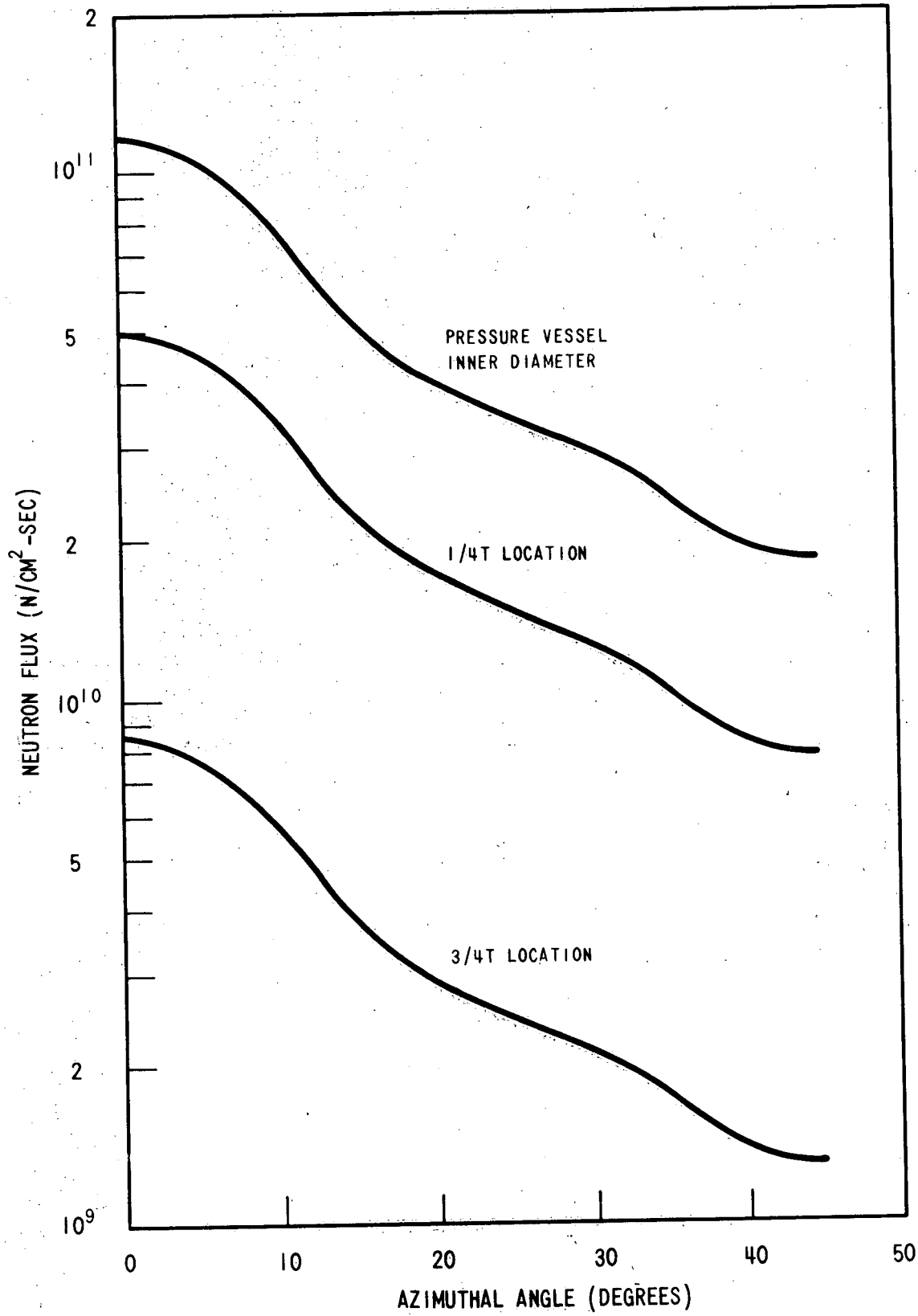


Figure 6-1. Calculated Azimuthal Distribution of Neutron Flux ($E > 1$ Mev) at the Core Midplane of the San Onofre Reactor Vessel

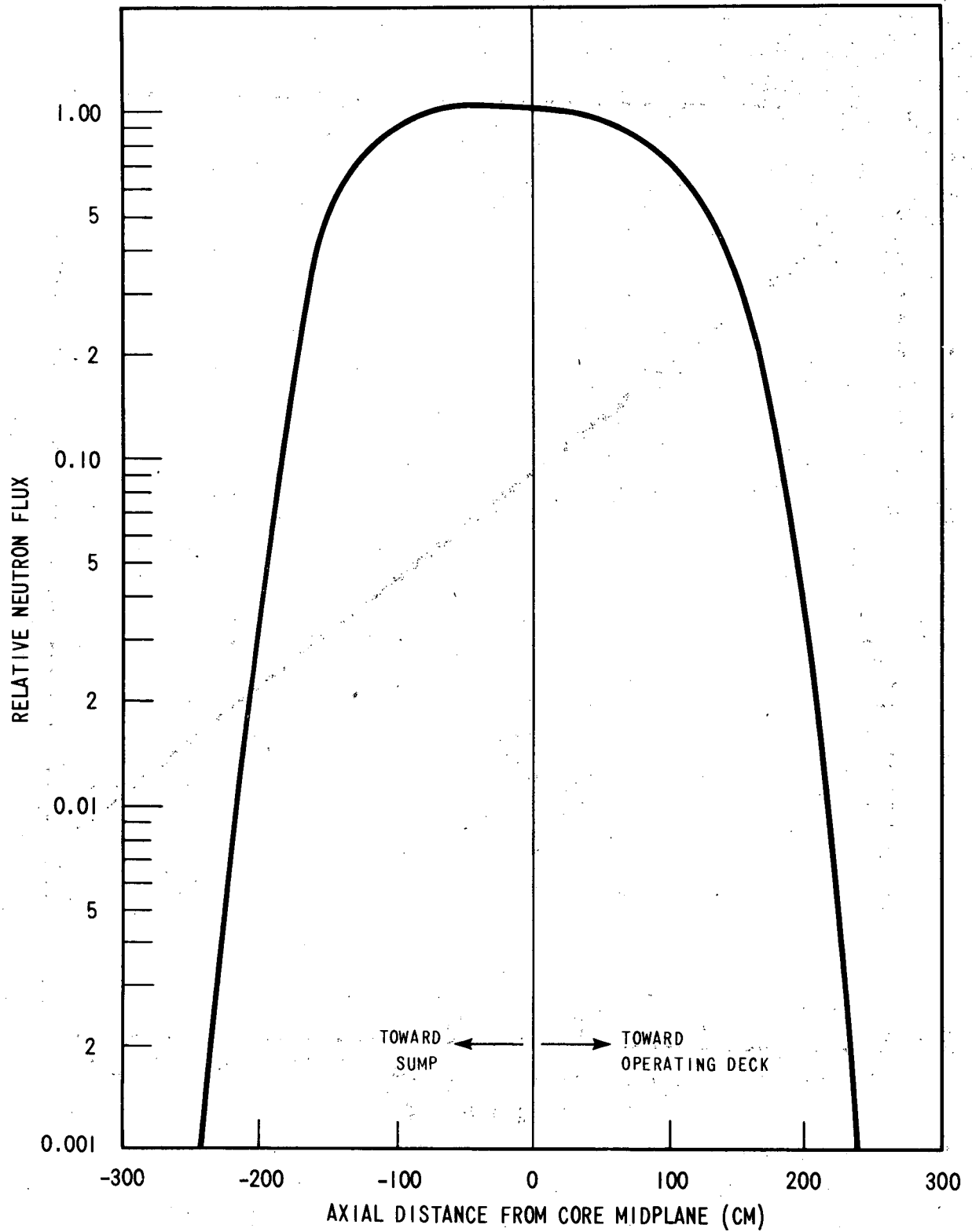


Figure 6-2. Relative Axial Variation of Fast Neutron Flux ($E > 1.0$ Mev) Incident on the San Onofre Reactor Vessel

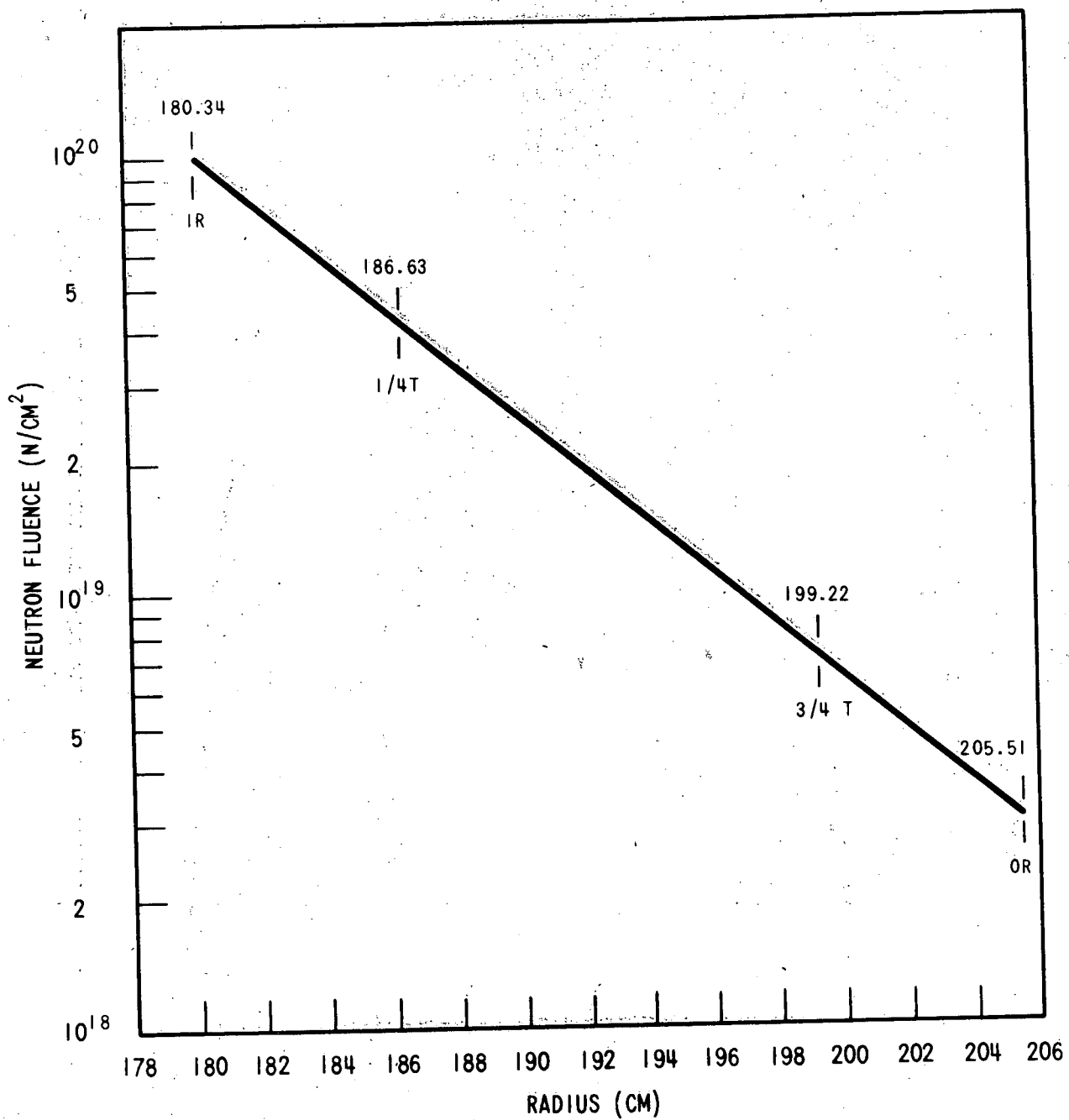


Figure 6-3. Calculated Maximum End-of-Life Fast Neutron Fluence ($E > 1$ Mev) as a Function of Radius Within the San Onofre Reactor Vessel

With the use of the lead factors listed in table 6-6, a comparison of the end-of-life peak fast neutron exposure of the San Onofre reactor as derived from both calculations and measured surveillance capsule results may be made as indicated in table 6-7.

TABLE 6-7
FAST NEUTRON EXPOSURE DERIVED FROM CALCULATED
AND MEASURED RESULTS

Vessel Location	Fast Neutron Fluence (n/cm ²)		
	Calculated	Based on Iron From Front Charpys	Based on Iron From Back Charpys
Inner Surface	1.0 x 10 ²⁰	1.0 x 10 ²⁰	1.1 x 10 ²⁰
1/4 Thickness	4.2 x 10 ¹⁹	4.2 x 10 ¹⁹	4.6 x 10 ¹⁹
3/4 Thickness	7.1 x 10 ¹⁸	7.1 x 10 ¹⁸	7.7 x 10 ¹⁸

These data are based on 27 full-power years of operation at 1347 Mw.

APPENDIX A

HEATUP AND COOLDOWN LIMIT CURVES FOR NORMAL OPERATION

A-1. INTRODUCTION

Heatup and cooldown limit curves are calculated using the most limiting value of RT_{NDT} (reference nil-ductility temperature). The most limiting RT_{NDT} of the material in the core region of the reactor vessel is determined by using the preservice reactor vessel material properties and estimating the radiation-induced ΔRT_{NDT} . RT_{NDT} is designated as the higher of the drop weight nil-ductility transition temperature (NDTT) or the temperature at which the material exhibits at least 50 ft lb of impact energy and 35-mil lateral expansion (normal to the major working direction) minus 60°F.

RT_{NDT} increases as the material is exposed to fast neutron radiation. Thus, to find the most limiting RT_{NDT} at any time period in the reactor's life, a ΔRT_{NDT} due to the radiation exposure associated with that time period must be added to the original unirradiated RT_{NDT} . The extent of the shift in RT_{NDT} is enhanced by certain chemical elements (such as copper) present in reactor vessel steels. Design curves which show the effect of fluence and copper content on ΔRT_{NDT} for reactor vessel steels exposed to 550°F are shown in figure A-1.

Given the copper content of the most limiting material, the radiation-induced ΔRT_{NDT} can be estimated from figure A-1. Fast neutron fluence ($E > 1$ Mev) at the vessel inner surface, the 1/4T (wall thickness) and 3/4T (wall thickness) vessel locations are given as a function of full-power service life in figure A-2. The data for all other ferritic materials in the reactor coolant pressure boundary are examined to assure that no other component will be limiting with respect to RT_{NDT} .

A-2. FRACTURE TOUGHNESS PROPERTIES

The preirradiation fracture toughness properties of the San Onofre Unit No. 1 reactor vessel materials are presented in table A-1. The fracture toughness properties of the ferritic material in the reactor coolant pressure boundary are determined in accordance with the NRC

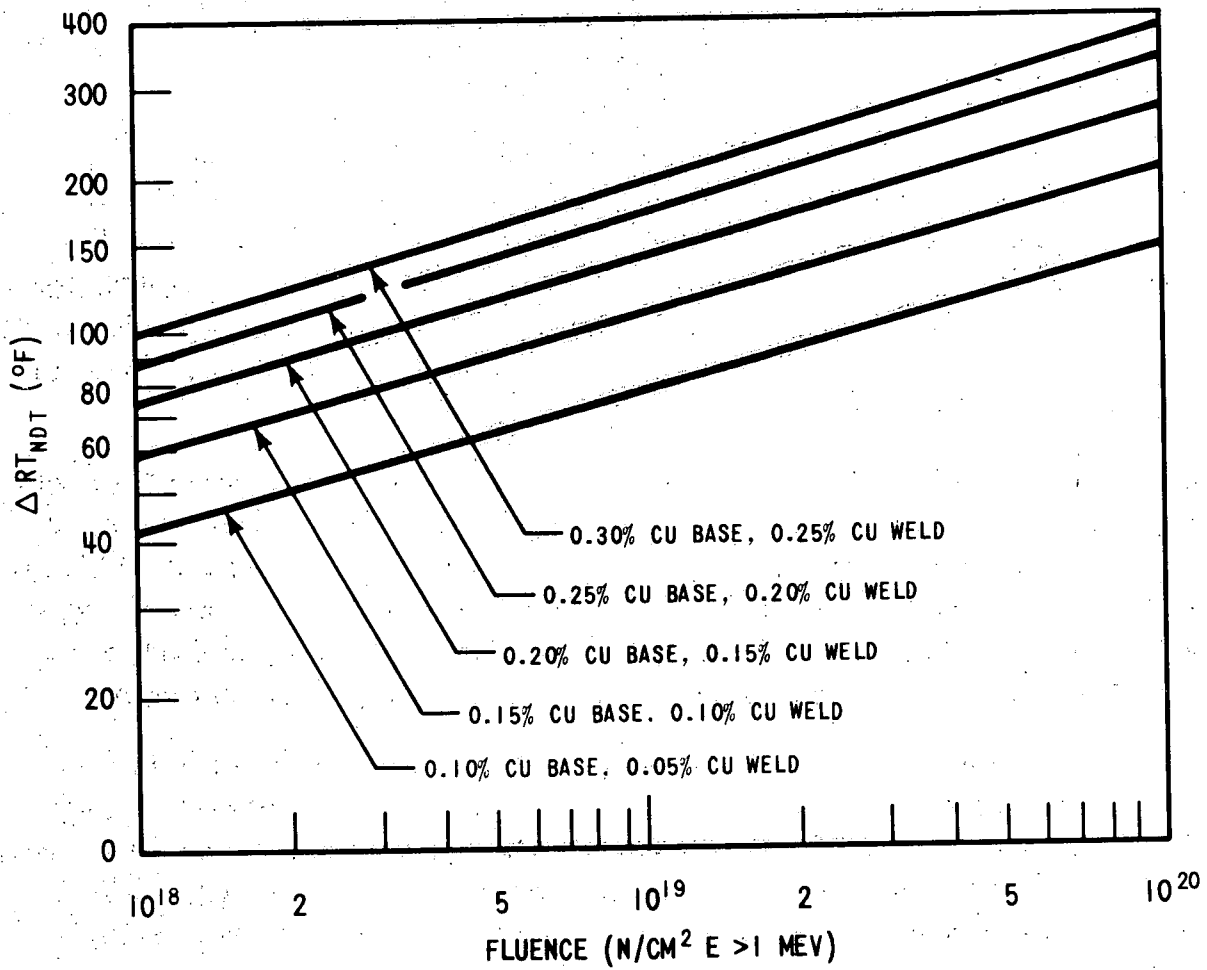


Figure A-1. Effect of Fluence and Copper Content on ΔRT_{NDT} for Reactor Vessel Steels Exposed to Irradiation at 550°F

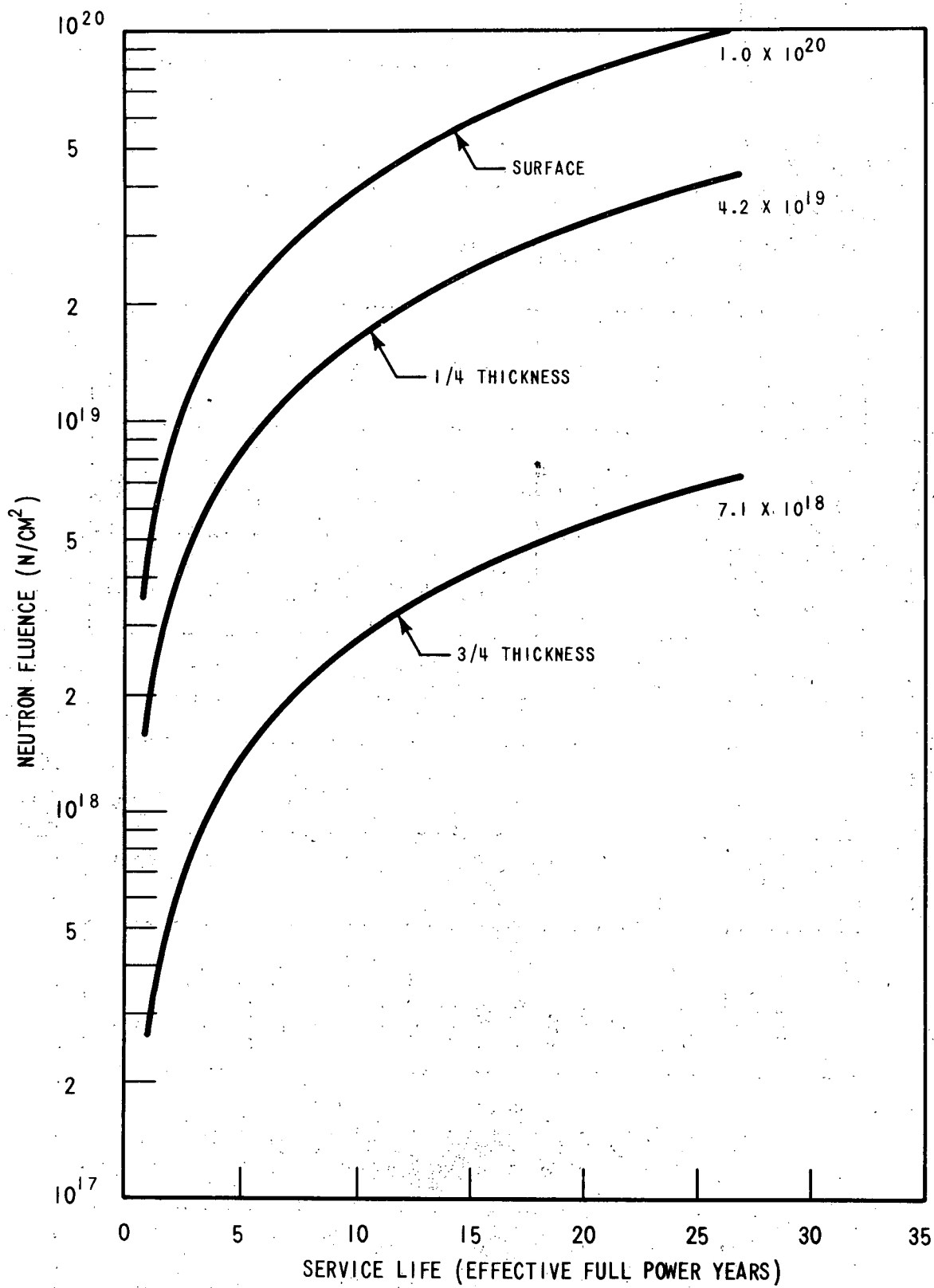


Figure A-2. Fast Neutron Fluence ($E > 1$ Mev) as a Function of Full-Power Service Life

TABLE A-1
REACTOR VESSEL TOUGHNESS DATA (UNIRRADIATED)

Component	Code No.	Material Type	Cu (%)	P (%)	NDTT (°F)	Minimum 50 ft-lb/35 mil Temp (°F)		RT _{NDT} (°F)	Average Upper Shelf Energy (ft-lb)	
						Long.	Trans.		Long.	Trans.
Cl. Hd. Dome	W7604	A302B	---	---	60 ^[a]	112	132	72	72.5	---
Peel Segment	W7605-1	A302B	---	---	-10	114	134	74	70.5	---
Peel Segment	W7605-2	A302B	---	---	-10	90	110	50	122	---
Peel Segment	W7605-3	A302B	---	---	-10	108	128	68	85	---
Peel Segment	W7605-4	A302B	---	---	-10	120	140	80	74	---
Peel Segment	W7605-5	A302B	---	---	-10	26	46	-10	109	---
Peel Segment	W7605-6	A302B	---	---	-10	102	122	62	88	---
Hd. Flange	W7602	A336 mod	---	---	60 ^[a]	[b]	---	60	---	---
Ves. Flange	W7603	A336 mod	---	---	60 ^[a]	[b]	---	60	---	---
Inlet Nozzle	W7611-1	A336 mod	---	---	60 ^[a]	[b]	---	60	---	---
Inlet Nozzle	W7611-2	A336 mod	---	---	60 ^[a]	[b]	---	60	---	---
Inlet Nozzle	W7611-3	A336 mod	---	---	60 ^[a]	[b]	---	60	---	---
Outlet Nozzle	W7610-1	A336 mod	---	---	60 ^[a]	[b]	---	60	---	---
Outlet Nozzle	W7610-2	A336 mod	---	---	60 ^[a]	[b]	---	60	---	---
Outlet Nozzle	W7610-3	A336 mod	---	---	60 ^[a]	[b]	---	60	---	---
Upper Shell	W7601-3	A302B	0.15	0.014	-10	48	68	8	98.5	---
Upper Shell	W7601-6	A302B	0.16	0.012	-30	64	84	24	104	---
Upper Shell	W7601-7	A302B	0.15	0.014	-20	52	72	12	95.5	---

a. Estimated per NRC Standard Review Plan Branch Technical Position MTEB 5-2.
b. Only 10°F Charpy V-notch data available. Conservative estimates for NDTT and RT_{NDT} were used.

A-4

TABLE A-1 (cont)
REACTOR VESSEL TOUGHNESS DATA (UNIRRADIATED)

Component	Code No.	Material Type	Cu (%)	P (%)	NDTT (°F)	Minimum 50 ft-lb/35 mil Temp (°F)		RT _{NDT} (°F)	Average Upper Shelf Energy (ft-lb)	
						Long.	Trans.		Long.	Trans.
Inter. Shell	W7601-1	A302B	0.17	0.013	0	57	120 ^[a]	60	94	75
Inter. Shell	W7601-8	A302B	0.18	0.012	10	93	100 ^[a]	40	97	79
Inter. Shell	W7601-9	A302B	0.18	0.014	0	64	115 ^[a]	55	102	72
Lower Shell	W7601-2	A302B	0.17	0.013	-20	74	94	34	97	---
Lower Shell	W7601-4	A302B	0.14	0.014	-10	91	111	51	94	---
Lower Shell	W7601-5	A302B	0.14	0.014	10	122	142	82	87.5	---
Bot. Hd. Peel	W7607	A302B	---	---	-20	62	82	22	91	---
Bot. Hd. Dome	W7606	A302B	---	---	60 ^[b]	99	119	60	86	---
Weld	---	---	0.19	0.017	0 ^[b]	---	29 ^[a]	0	---	90
HAZ	---	---	---	---	0 ^[b]	---	-14 ^[a]	0	---	101

a. Actual not estimated

b. Estimated per NRC Standard Review Plan Branch Technical Position MTEB 5-2.

Regulatory Standard Review Plan.^[1] The postirradiation fracture toughness properties of the reactor vessel belt line material were obtained directly from the San Onofre Unit No. 1 Vessel Material Surveillance Program.

A-3. CRITERIA FOR ALLOWABLE PRESSURE-TEMPERATURE RELATIONSHIPS

The ASME approach for calculating the allowable limit curves for various heatup and cooldown rates specifies that the total stress intensity factor, K_I , for the combined thermal and pressure stresses at any time during heatup or cooldown cannot be greater than the reference stress intensity factor, K_{IR} , for the metal temperature at that time. K_{IR} is obtained from the reference fracture toughness curve, defined in Appendix G to the ASME Code.^[2] The K_{IR} curve is given by the equation:

$$K_{IR} = 26.78 + 1.223 \exp [0.0145 (T - RT_{NDT} + 160)] \quad (A-1)$$

where K_{IR} is the reference stress intensity factor as a function of the metal temperature T and the metal reference nil-ductility temperature RT_{NDT} . Thus, the governing equation for the heatup-cooldown analysis is defined in Appendix G to the ASME Code^[2] as follows:

$$C K_{IM} + K_{It} \leq K_{IR} \quad (A-2)$$

where

K_{IM} is the stress intensity factor caused by membrane (pressure) stress.

K_{It} is the stress intensity factor caused by the thermal gradients.

K_{IR} is a function of temperature relative to the RT_{NDT} of the material.

$C = 2.0$ for Level A and Level B Service Limits.

$C = 1.5$ for Hydrostatic and Leak test conditions during which the reactor core is not critical.

At any time during the heatup or cooldown transient, K_{IR} is determined by the metal temperature at the tip of the postulated flaw, the appropriate value for RT_{NDT} , and the reference fracture toughness curve. The thermal stresses resulting from temperature gradients through the

1. "Fracture Toughness Requirements for Older Plants" Branch Technical Position MTEB 5-2 Standard Review Plan, NUREG-75/087, 1975.

2. Appendix G to the ASME Boiler and Pressure Vessel Code, Section III, Division 1, Subsection NA, "Protection Against Non-Ductile Failure," American Society of Mechanical Engineers, New York, N.Y., 1977 Edition and Summer 1978 Addenda.

vessel wall are calculated and then the corresponding (thermal) stress intensity factors, K_{I_t} , for the reference flaw are computed. From equation (A-2) the pressure stress intensity factors are obtained, and from these the allowable pressures are calculated.

For the calculation of the allowable pressure versus coolant temperature during cooldown, the code reference flaw is assumed to exist at the inside of the vessel wall. During cooldown, the controlling location of the flaw is always at the inside of the wall because the thermal gradients produce tensile stresses at the inside, which increase with increasing cooldown rates. Allowable pressure-temperature relations are generated for both steady-state and finite cooldown rate situations. From these relations composite limit curves are constructed for each cooldown rate of interest.

The use of the composite curve in the cooldown analysis is necessary because control of the cooldown procedure is based on measurement of reactor coolant temperature, whereas the limiting pressure is actually dependent on the material temperature at the tip of the assumed flaw. During cooldown, the 1/4T vessel location is at a higher temperature than the fluid adjacent to the vessel ID. This condition, of course, is not true for the steady-state situation. It follows that at any given reactor coolant temperature, the ΔT developed during cooldown results in a higher value of K_{I_R} at the 1/4T location for finite cooldown rates than for steady-state operation. Furthermore, if conditions exist such that the increase in K_{I_R} exceeds K_{I_t} , the calculated allowable pressure during cooldown will be greater than the steady-state value.

The above procedures are needed because there is no direct control on temperature at the 1/4T location; therefore, allowable pressures may unknowingly be violated if the rate of cooling is decreased at various intervals along a cooldown ramp. The use of the composite curve eliminates this problem and assures conservative operation of the system for the entire cooldown period.

Three separate calculations are required to determine the limit curves for finite heatup rates. As is done in the cooldown analysis, allowable pressure-temperature relationships are developed for steady-state conditions as well as finite heatup rate conditions assuming the presence of a 1/4T defect at the inside of the vessel wall. The thermal gradients during heatup produce compressive stresses at the inside of the wall that alleviate the tensile stresses produced by internal pressure. The metal temperature at the crack tip lags the coolant temperature; therefore, the K_{I_R} for the 1/4 crack during heatup is lower than the K_{I_R} for the 1/4T crack during steady-state conditions at the same coolant temperature. During heatup, especially at the end of the transient, conditions may exist such that the effects of compressive thermal stresses and lower K_{I_R} 's do not offset each other, and the pressure-temperature curve based on steady-state

conditions no longer represents a lower bound of all similar curves for finite heatup rates when the 1/4T flaw is considered. Therefore, both cases have to be analyzed in order to assure that at any coolant temperature the lower value of the allowable pressure calculated for steady-state and finite heatup rates is obtained.

The second portion of the heatup analysis concerns the calculation of pressure-temperature limitations for the case in which a 1/4T deep outside surface flaw is assumed. Unlike the situation at the vessel inside surface, the thermal gradients established at the outside surface during heatup produce stresses which are tensile in nature and thus tend to reinforce any pressure stresses present. These thermal stresses are dependent on both the rate of heatup and the time (or coolant temperature) along the heatup ramp. Since the thermal stresses at the outside are tensile and increase with increasing heatup rates, each heatup rate must be analyzed on an individual basis.

Following the generation of pressure-temperature curves for both the steady-state and finite heatup rate situations, the final limit curves are produced as follows. A composite curve is constructed based on a point-by-point comparison of the steady-state and finite heatup rate data. At any given temperature, the allowable pressure is taken to be the lesser of the three values taken from the curves under consideration.

The use of the composite curve is necessary to set conservative heatup limitations because it is possible for conditions to exist such that over the course of the heatup ramp the controlling condition switches from the inside to the outside and the pressure limit must at all times be based on analysis of the most critical criterion.

Finally, the composite curves for the heatup rate data and the cooldown rate data are adjusted for possible errors in the pressure and temperature sensing instruments by the values indicated on the respective curves.

A-4. HEATUP AND COOLDOWN LIMIT CURVES

Limit curves for normal heatup and cooldown of the primary Reactor Coolant System have been calculated using the methods discussed in paragraph A-3. The derivation of the limit curves is presented in the NRC Regulatory Standard Review Plan.^[1]

Transition temperature shifts occurring in the pressure vessel materials due to radiation exposure have been obtained directly from the reactor pressure vessel surveillance program.

1. "Pressure Temperature Limits," Section 5.3.2 of Standard Review Plan, NUREG-75/087, 1975.

Charpy test specimens from Capsule F indicate that the representative core region weld metal and the limiting core region plate (W7601-8) exhibited shifts in RT_{NDT} of 165° and $110^{\circ}F$, respectively. These shifts at a fluence of $5.14 \times 10^{19} \text{ n/cm}^2$ are well within the appropriate design curve (figure A-1) prediction. Heatup and cooldown calculations were based on the ΔRT_{NDT} predicted for the core region plate material which is considered to be the limiting vessel material. Heatup and cooldown limit curves for normal operation of the reactor vessel are presented in figures A-3 and A-4 and represent an operational time period of 16 effective full power years.

Allowable combinations of temperature and pressure for specific temperature change rates are below and to the right of the limit lines shown on the heatup and cooldown curves. The reactor must not be made critical until pressure-temperature combinations are to the right of the criticality limit line shown in figure A-3, in addition to other criteria which must be met before the reactor is made critical.

The leak test limit curve shown in figure A-3 represents minimum temperature requirements at the leak test pressure specified by applicable codes. The leak test limit curve was determined by methods of references 1 and 2:

Figures A-3 and A-4 define limits to assure prevention of nonductile failure.

Since plant heatup and cooldown limitations were re-evaluated using the new peak fast fluence values resulting from the analyses performed on Capsule F and updated estimates of RT_{NDT} , sections of the plant Technical Specifications which address plant heatup and cooldown limitations should be amended to reflect the changes in normal plant operation limitations.

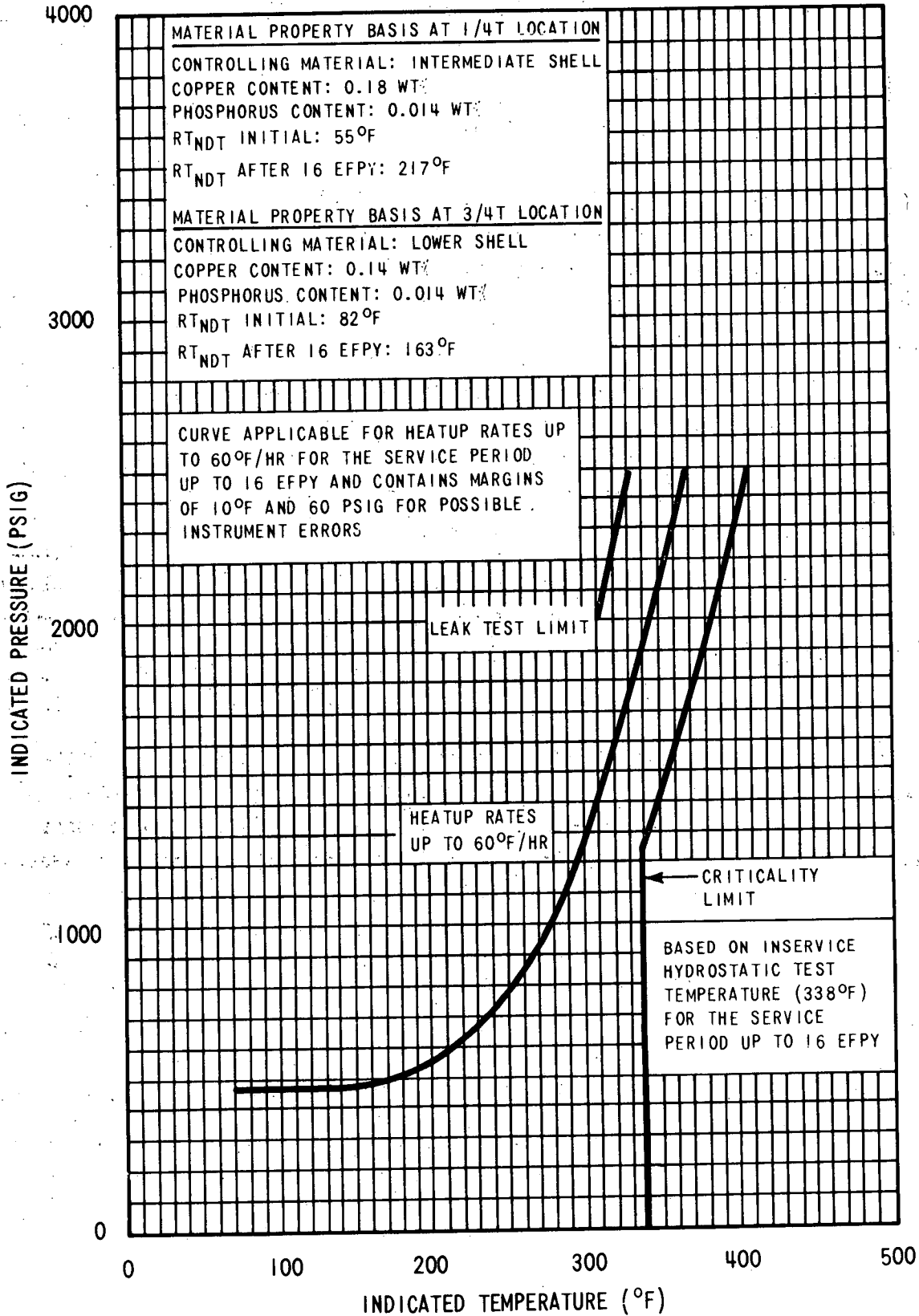


Figure A-3. San Onofre Unit No. 1 Reactor Coolant System Heatup Limitations Applicable for the First 16 EFY

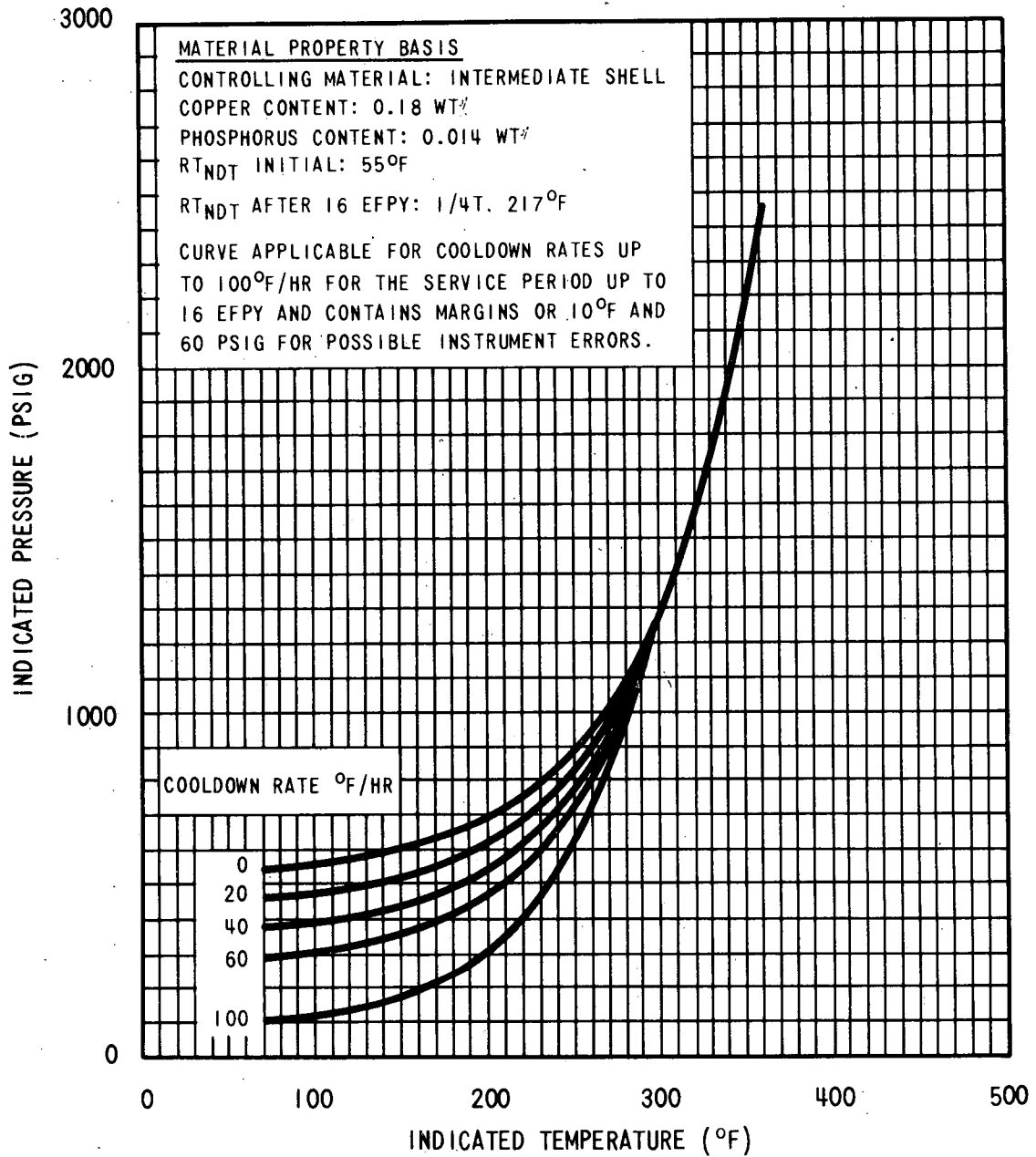


Figure A-4. San Onofre Unit No. 1 Reactor Coolant System
 Cooldown Limitations Applicable for the First
 16 EFY